AD_____

Award Number: W81XWH-05-1-0300

TITLE: Structural Characterization and Determinants of Specificity of Single-Chain Antibody Inhibitors of Membrane-Type Serine Protease 1

PRINCIPAL INVESTIGATOR: Christopher J. Farady

CONTRACTING ORGANIZATION: University of California
San Francisco, CA 94143-2280

REPORT DATE: March 2007

TYPE OF REPORT: Annual Summary

PREPARED FOR: U.S. Army Medical Research and Materiel Command
Fort Detrick, Maryland 21702-5012

REPORT DOCUMENTATION PAGE

Form Approved
OMB No. 0704-0188

1. REPORT DATE *(DD-MM-YYYY)*	**2. REPORT TYPE**	**3. DATES COVERED** *(From - To)*
01/03/07	Annual Summary	21 Feb 2006 – 20 Feb 2007

4. TITLE AND SUBTITLE

Structural Characterization and Determinants of Specificity of Single- Chain Antibody Inhibitors of Membrane-Type Serine Protease 1

5a. CONTRACT NUMBER

5b. GRANT NUMBER
W81XWH-05-1-0300

5c. PROGRAM ELEMENT NUMBER

6. AUTHOR(S)
Christopher J. Farady

E-Mail: christopher.farady@ucsf.edu

5d. PROJECT NUMBER

5e. TASK NUMBER

5f. WORK UNIT NUMBER

7. PERFORMING ORGANIZATION NAME(S) AND ADDRESS(ES)

University of California
San Francisco, CA 94143-2280

8. PERFORMING ORGANIZATION REPORT NUMBER

9. SPONSORING / MONITORING AGENCY NAME(S) AND ADDRESS(ES)
U.S. Army Medical Research and Materiel Command
Fort Detrick, Maryland 21702-5012

10. SPONSOR/MONITOR'S ACRONYM(S)

11. SPONSOR/MONITOR'S REPORT NUMBER(S)

12. DISTRIBUTION / AVAILABILITY STATEMENT
Approved for Public Release; Distribution Unlimited

13. SUPPLEMENTARY NOTES

14. ABSTRACT: Membrane-type serine protease 1 (MT-SP1) is a cancer-associated serine protease implicated in the tumorogenesis and metastasis of breast cancer. Inhibition of MT-SP1 activity has been shown to decrease metastatic potential. We have developed a number of potent and specific single-chain (scFv) antibody inhibitors to MT-SP1, and have begun to characterize their mechanism of inhibition. Through kinetic characterization and site-directed mutagenesis experiments, it has been determined that three potent inhibitors have separate and novel mechanisms of inhibition which do not mimic either biologically or pharmaceutically relevant protease inhibitors. These novel modes of binding and inhibition are the basis for their specificity, and suggest these inhibitors will have less cross-reactivity and toxicity problems when used in vivo to further dissect the role of MT-SP1 in breast cancer.

15. SUBJECT TERMS
Antibody inhibitors, Proteases in cancer, Protease specificity

16. SECURITY CLASSIFICATION OF:			**17. LIMITATION OF ABSTRACT**	**18. NUMBER OF PAGES**	**19a. NAME OF RESPONSIBLE PERSON**
a. REPORT	**b. ABSTRACT**	**c. THIS PAGE**			USAMRMC
U	U	U	UU	25	**19b. TELEPHONE NUMBER** *(include area code)*

Table of Contents

Introduction:

My research has focused on the mechanism of inhibition of a set of single-chain inhibitors of Membrane-Type Serine Protease 1 (MT-SP1). MT-SP1 is a type II transmembrane serine protease (TTSP) expressed on the surface of epithelial cells. Research over the past 10 years have shown that MT-SP1 is involved in a number of biological processes, including tissue development, cell adhesion, and growth factor activation. Furthermore, a number of experiments have suggested dysregulated MT-SP1 activity may have a critical role in tumor progression and metastasis (Uhland 2006). Immunoblotting, immunohistochemical analysis, and expression level analysis have found MT-SP1 to be differentially overexpressed in breast, prostate, and ovarian cancers. MT-SP1 has been shown to play a role in ovarian (Suzuki et al. 2004) and prostate (Galkin et al. 2004) tumor invasion using experimental methods including inhibition of MT-SP1 by small molecules and anti-sense. In breast cancer, MT-SP1 expression levels, when correlated with substrate expression levels have been prognostic in disease progression. High levels of MT-SP1 expression has been correlated with the expression of hepatocyte growth factor (HGF) and the Met/HGF receptor (Kang et al 2003), and with the glycosylation enzyme β1,6-N-Acetylglucosaminyltransferase V (Siddiqui et al. 1999), and in both cases, these clusters showed prognostic value for disease-related survival. MT-SP1 expression levels have also been correlated with macrophage stimulating protein (MSP) (Bhatt et al, 2007), and co-expression of MT-SP1, MSP, and its receptor, RON, have been implicated in breast cancer metastasis to the bone (Welm et al. 2007). Finally, modest orthotopic overexpression of MT-SP1 in mouse epidermal tissue led to spontaneous squamous cell carcinomas (List et al. 2005), further cementing MT-SP1's role in cancer, and suggesting the enzyme is causally involved in malignant transformation.

In order to tease apart the role of MT-SP1 in tumor progression, the Craik Lab has used phage display to develop a series of potent and specific single-chain antibody inhibitors (scFv) of the catalytic domain of MT-SP1 (Sun et al. 2003). With K_i's ranging from 10pM to 10nM, these inhibitors are extremely potent *in vitro*, and showed no appreciable inhibition of a panel of closely related serine proteases including factor Xa, thrombin, kallikrein, tPA, and uPA. The potential benefits of these inhibitors are two-fold: they can be used to probe complex biology of MT-SP1, both its role in normal and cancer biology, and they can be used to validate MT-SP1 as both an imaging and therapeutic target. From a more biophysical standpoint, these inhibitors are unique in that they are the only reported antibody inhibitors of serine proteases, a large class of homologous enzymes in which the development of specific inhibitors has been a monumental challenge. Most protease inhibitors take advantage of either the catalytic machinery or topological fold of the protease. These scFv inhibitors bind and recognize a specific three-dimensional epitope near the active site of the enzyme, which allows for specificity among proteases, and allows for a fundamentally different mechanism of inhibition from other biologically active protease inhibitors. A thorough understanding of the mechanism of inhibition of these inhibitors will help us validate their putative mode of action *in vivo*, and will suggest new strategies for inhibition of MT-SP1 and other serine proteases.

Results:

Significant progress has been made in my aims of kinetically and structurally characterizing the interactions between two potent scFv inhibitors of MT-SP1, named E2, S4. Using a combination of mutagenesis experiments, steady state kinetics, and stopped flow kinetics, we have determined the mechanism of inhibition of both of these novel macromolecular inhibitors. These results have recently been published in the *Journal of Molecular Biology* and are attached in appendix 1.

S4 is a competitive inhibitor of MT-SP1 with a K_I of 140pM, and a number of kinetic competition experiments have shown it binds at or near the S1-site in the protease active site, which is critical to substrate and inhibitor binding. The scFv has a fast association rate, of $1.2x10^8$ $M^{-1}s^{-1}$, nearly an order of magnitude faster than that of a typical protein-protein interaction. It has a one-step binding mechanism, and rapidly comes to binding equilibrium with the protease. The surface loops of closely related serine proteases surround the protease active site and show a high degree of sequential diversity. Alanine scanning these loops has helped define the binding epitope of the antibody, and thus the basis of its specificity. S4 makes a number of moderate interactions with the six loops surrounding the protease active site, effectively capping the active site and preventing substrate binding.

E2 has a more complex mechanism of inhibition. It too is a competitive inhibitor of MT-SP1, has a K_I of 8.0pM, and competes with substrate binding in the active site. Stopped-flow experiments revealed that there are at least two binding steps in the inhibition process, suggesting E2 is a mechanistic inhibitor of MT-SP1. Digest experiments show that E2 binds in the protease active site in a substrate-like manner, and can be cleaved like a substrate-like manner. The multiple binding steps and the substrate-like binding suggest that E2 is a standard mechanism serine protease inhibitor. Standard mechanism serine protease inhibitors are ubiquitous in nature, and this mechanism is used to modulate nearly all serine proteases. Despite their robustness, though, standard mechanism inhibitors, such as bovine pancreatic trypsin inhibitor (BPTI), are not specific, and can inhibit many serine proteases. E2 shows a high degree of specificity, though. Alanine scanning of the surface loops of the protease reveal that E2 gains its binding specificity through interactions with the 90's loop of MT-SP1. Mutations of F97 and D96 to alanine nearly abolish E2 binding to the protease. Therefore, E2 is a standard mechanism inhibitor that gains its specificity from its interaction with a 'hot-spot' centered on the 90's loop of MT-SP1.

The significance of these results are two-fold. The mechanisms of inhibition provide a rationale for the effectiveness of these inhibitors, and suggest that the development of specific antibody-based inhibitors against individual members of closely related enzyme families is feasible, and an effective way to develop tools to tease apart complex biological processes. Furthermore, it suggests that these inhibitors might be effective *in vivo* tools, either as biological inhibitors of MT-SP1, or as imaging or detection tools. E2 has been used as a tool to validate the growth factor MSP as a substrate of MT-SP1. E2 inhibited MT-SP1 on the surface of mouse peritoneal macrophages, and prevented the processing of pro-MSP, and the resulting activation of the macrophages (appendix 2). This helps provide evidence for a signaling axis consisting of MT-SP1, MSP, and its receptor, RON, which appears to be important in directing breast cancer metastases to the bone.

Future Directions

My proposal aimed to crystallize the MT-SP1-inhibitor complex of the inhibitors. To date, despite setting up more than 1,500 crystallization conditions, I have not been able to get crystals that diffract to more than 8 angstroms. In an effort to improve the chances of crystallization, I plan on converting the antibodies to an Fab scaffold. There are also a number of surface residue mutations - such as removing cysteines - that have been designed that might improve the behavior of MT-SP1 in solution and make the complex more amenable to crystallization.

Key Research and Training Accomplishments:

- Determined the modes and mechanisms of inhibition of the two most potent scFv inhibitors of the breast-cancer associated serine protease MT-SP1. These results have been summarized in the manuscript "The Mechanism of Inhibition of Antibody-Based Inhibitors of Membrane-Type Serine Protease 1 (MT-SP1)", which has been accepted by the *Journal of Molecular Biology* (see Reportable Outcomes and Appendix 1).

- The scFv inhibitor EB-9 has been validated as a useful biological tool in cell-culture assays; it inhibited MT-SP1 activity on the surface of mouse peritoneal macrophages. These results were published in "Coordinate expression and functional profiling identify an extracellular proteolytic signaling pathway" in the *Proceedings of the National Academy of Sciences* (see Reportable Outcomes and Appendix 2).

- Attended and presented a peer-reviewed poster of this work at the Gordon Conference on "Proteases and their Inhibitors", in July 2006.

- Registered for and will present a poster at the 2007 UCSF Breast Oncology Program annual conference. This two-day retreat this year is focused on molecular diagnostics, the UCSF Early Detection Research Program; the Integrative Cancer Biology Program.

Reportable Outcomes:

Two papers have been accepted for publication in the past year.

- Bhatt, AS, Welm, A, Farady, CJ, Vasquez, M, Wilson, K, and Craik, CS. (2007). Coordinate expression and functional profiling identify an extracellular proteolytic signaling pathway. *Proc Natl Acad Sci U S A* **104**, 5771-5776.
- Farady, CJ, Sun, J, Darragh, MR, Miller, SM, and Craik, CS. (2007). The mechanism of inhibition of antibody-based inhibitors of Membrane-Type Serine Protease 1 (MT-SP1). *J Mol Biol* in press.

Future results outlined above will be reportable, and will be published when experiments are completed.

References:

Galkin AV, Mullen L, Fox WD, Brown J, Duncan D, Moreno O, Madison EL. CVS-3983, a selective matriptase inhibitor, suppresses the growth of androgen independent prostate tumor xenografts. *The Prostate* 2004, **61,** 228-35.

Kang JY, Dolled-Filhart M, Ocal IT, Singh B, Lin CY, Dickson RB, Lim DL, Camp RL. Tissue microarray analysis of hepatocyte growth factor/met pathway components reveals a role for met, matriptase, and HGF-HAI1 in the progression of node-negative breast cancer. *Cancer Research* 2003, **63**, 1101-5.

Lin CY, Anders J, Johnson M, Dickson RB. Purification and characterization of a complex containing matriptase and a Kunitz-type serine protease inhibitor from human milk. *Journal of Biological Chemistry* 1999, **274**, 18237-42.

List K, Szabo R, Molinolo A, Sriuranpong V, Redeye V, Murdock T, Burke B, Nielsen BS, Gutkind JS, Bugge TH. Deregulated matriptase causes ras-independent multistage carcinogenesis and promotes ras-mediated malignant transformation. *Genes Dev* 2005, **16**, 1934-50.

Sun J, Pons J, Craik CS. Potent and selective inhibition of membrane-type serine protease 1 by human single-chain antibodies. *Biochemistry* 2003, **42**, 892-900.

Suzuki M, Kobayashi H, Kanayama N, Saga Y, Suzuki M, Lin CY, Dickson RB, Terao T. Inhibition of tumor invasion by genomic down-regulation of matriptase through suppression of activation of receptor-pound pro-urokinase. *Journal of Biological Chemistry* 2004, **279**, 14899-908.

Takeuchi T, Shuman MA, Craik CS. Reverse biochemistry: use of macromolecular protease inhibitors to dissect complex biological processes and identify a membrane-type serine protease in epithelial cancer and normal tissue. *Proc Natl Acad Sci U S A* 1999, **96**, 11054-61.

doi:10.1016/j.jmb.2007.03.078 J. Mol. Biol. (2007) xx, xxx–xxx

JMB

Available online at www.sciencedirect.com
ScienceDirect

ELSEVIER

The Mechanism of Inhibition of Antibody-based Inhibitors of Membrane-type Serine Protease 1 (MT-SP1)

Christopher J. Farady[1], Jeonghoon Sun[2], Molly R. Darragh[1] Susan M. Miller[1] and Charles S. Craik[1,2*]

[1]*Graduate Group in Biophysics University of California San Francisco, 600 16th St. Genentech Hall, San Francisco CA. 94143, USA*

[2]*Department of Pharmaceutical Chemistry, University of California, San Francisco 600 16th St. Genentech Hall San Francisco, CA. 94143, USA*

**Corresponding author*

The mechanisms of inhibition of two novel scFv antibody inhibitors of the serine protease MT-SP1/matriptase reveal the basis of their potency and specificity. Kinetic experiments characterize the inhibitors as extremely potent inhibitors with K_I values in the low picomolar range that compete with substrate binding in the S1 site. Alanine scanning of the loops surrounding the protease active site provides a rationale for inhibitor specificity. Each antibody binds to a number of residues flanking the active site, forming a unique three-dimensional binding epitope. Interestingly, one inhibitor binds in the active site cleft in a substrate-like manner, can be processed by MT-SP1 at low pH, and is a standard mechanism inhibitor of the protease. The mechanisms of inhibition provide a rationale for the effectiveness of these inhibitors, and suggest that the development of specific antibody-based inhibitors against individual members of closely related enzyme families is feasible, and an effective way to develop tools to tease apart complex biological processes.

Keywords: antibody; standard mechanism protease inhibitor; specificity; serine protease; HuCAL

Introduction

Of the 22 families of naturally occurring, protein-based protease inhibitors known to inhibit the S1 clan of serine proteases, 18 use an identical mechanism of inhibition.[1] Standard mechanism (also known as canonical, or Laskowski mechanism) inhibitors all insert a reactive loop into the active site of the protease, which binds in an extended β-sheet in a substrate-like manner.[2] While some of these inhibitors have developed secondary mechanisms,[3] the primary mechanism of inhibition is extremely well conserved; so much so that crystal structures of unrelated inhibitors overlay perfectly in the protease active site.[4] As evidenced by this remarkable example of convergent evolution, the standard mechanism is an efficient, robust way to inhibit serine proteases. However, this robustness often comes at the expense of specificity. With the exception of a small number of parasitic anti-thrombin inhibitors that also bind to protease exosites,[5] the majority of standard mechanism protease inhibitors have a relatively broad specificity. Bovine pancreatic trypsin inhibitor (BPTI) inhibits efficiently almost all trypsin-fold serine proteases with P1-Arg specificity, but can inhibit chymotrypsin (P1-Phe specificity) with a K_I of 10 nM.[6]

Much effort has been expended on the development of specific protease inhibitors for use both as biological tools and as potential therapeutic agents. As attempts to make specific small molecules have beset by difficulties,[7] researchers have often attempted to gain specificity using peptide or protein-based scaffolds. Constrained peptide phage display libraries have yielded extremely potent exosite inhibitors of factor VIIa,[8,9] and standard mechanism inhibitors of chymotrypsin,[10] and urokinase-type plasminogen activator (uPA),[11] with moderate potency and specificity. An alternate approach has

Present address: J. Sun, Amgen Inc., Thousand Oaks, CA. 91320, USA.

Abbreviations used: BPTI, bovine pancreatic trypsin inhibitor; uPA, urokinase-type plasminogen activator; scFv, single-chain variable fragment; MT-SP1, membrane-type serine protease 1; HuCAL, human combinatorial antibody library; pNA, *para*-nitroanilide; pAB, *p*-aminobenzamidine; ESI, electron spray ionization.

E-mail address of the corresponding author: craik@cgl.ucsf.edu

0022-2836/$ - see front matter © 2007 Published by Elsevier Ltd.

Please cite this article as: Farady, C. J. *et al.*, The Mechanism of Inhibition of Antibody-based Inhibitors of Membrane-type Serine Protease 1 (MT-SP1), *J. Mol. Biol.* (2007), doi:10.1016/j.jmb.2007.03.078

been to improve the specificity of naturally occurring protease inhibitors.[12–14] For example, maturation of Alzheimer's amyloid β-protein precursor inhibitor Kunitz domain, a canonical serine protease inhibitor, *via* competitive phage display improved its specificity for factor VIIa by increasing its K_I against a panel of some related serine proteases by two to five orders of magnitude.[13] A third approach has been to mature specific protease inhibitors on other natural protein scaffolds, such as ankyrin repeats or antibodies.[15] Until now, the characterized protease antibody inhibitors have been monoclonal antibodies raised from hybridomas, and have tended towards two types of inhibitors; those that interfere with multimerization (and thus activation) of the protease,[16–18] and those that bind to loops and protein–protein interaction sites[19–22] and occlude substrate binding, instead of interfering with the catalytic machinery of the enzyme, and ensuring complete inhibition.[23]

Earlier, we reported the development of single-chain variable fragment (scFv) antibody inhibitors of the serine protease membrane-type serine protease 1 (MT-SP1).[24] MT-SP1 (also called matriptase) was discovered and cloned in a search for serine proteases expressed in the PC-3 prostate cancer cell line,[25] and was determined independently to be a highly expressed protease in breast cancer tissue.[26] Work by a number of groups has since shown that MT-SP1 may be a key upstream factor involved in the ECM remodeling, and in signal transduction cascades involved in cell transformation.[27] Ablation of MT-SP1 activity has been shown to decrease the invasiveness of both ovarian and prostate tumor cells, and modest orthotopic over-expression of MT-SP1 in mouse epidermal tissue led to spontaneous squamous cell carcinomas,[28] further cementing the role of MT-SP1s in cancer, and suggesting the enzyme is causally involved in malignant transformation.

Here, we have characterized the mechanism of inhibition of the two most potent scFv inhibitors of MT-SP1, E2 and S4. The inhibitors were selected from a fully synthetic human combinatorial antibody library in the scFv format (HuCAL, MorphoSys AG). HuCAL-scFv contains consensus frameworks with diversified light and heavy chain CDR3 regions reflecting the natural human amino acid composition.[29] A combination of mutagenesis experiments, steady-state kinetics, and stopped-flow kinetics reveal that, while the inhibitors gain specificity by making a number of critical interactions with surface loops on the protease, they can be standard mechanism inhibitors, which insert a reactive loop in a substrate like manner into the active site of the protease. This work suggests that the antibody scaffold can be used to create extremely specific standard mechanism protease inhibitors. Furthermore, the design of inhibitors that utilize macromolecular recognition factors (variable loops, protein–protein interaction sites) can help to differentiate highly homologous proteases, and can thus impart specificity upon the inhibitors.

Results

Earlier, we described the maturation and initial characterization of a number of scFv inhibitors of MT-SP1.[24] The scFvs bound tightly to the catalytic domain of MT-SP1, and showed a high degree of specificity, as they showed no appreciable inhibition of a panel of closely related serine proteases, including factor Xa, thrombin, kallikrein, tissue plasminogen activator (tPA), and uPA at inhibitor concentrations of 1 μM. Here, we characterize the mechanism of inhibition of E2 and S4, the two most potent members of this novel class of serine protease inhibitors.

Steady-state kinetics

Previous experiments showed that E2 and S4 had K_D values of 160 pM and 500 pM (as determined by surface plasmon resonance), and were potent inhibitors of MT-SP1. In the current study, a number of steady-state kinetic experiments were performed in an attempt to understand the mechanism of inhibition of these inhibitors. The results of these experiments are summarized in Table 1. Double reciprocal plots revealed that both E2 and S4 are competitive inhibitors of MT-SP1 with respect to Spectrazyme-tPA, a small molecule *para*-nitroanilide (pNA) substrate of P1 arginine serine proteases. To further characterize the tight-binding nature of these inhibitors, accurate K_I values were determined; E2 and S4 are extremely tight-binding competitive inhibitors of MT-SP1, with K_I values of 8.0(±1.3) pM and 140(±6.0) pM, respectively.

To verify that the mode of inhibition is similar in the context of a macromolecular substrate, a discontinuous assay was developed to measure the activation of uPA. The K_M of uPA as a substrate for MT-SP1 was determined to be 1.7(±0.2) μM, and the k_{cat} of MT-SP1 activation of sc-uPA was 0.89(±0.09) s^{-1}. Double reciprocal plots showed that the inhibitors were indeed competitive with respect to macromo-

t1.2 **Table 1.** Kinetic parameters of scFv inhibitors

t1.3		k_{on}[a] ($10^6 M^{-1}s^{-1}$)	k_{off}[a] ($10^{-3}s^{-1}$)	K_d[a] (nM)	Mode of inhibition	K_i (pM)	Macromolecular MOI	Macromolecular K_i (pM)
t1.4	E2	2.1	0.38	0.16	Competitive	8.0±1.3	Competitive	12
t1.5	S4	11.5	5.8	0.51	Competitive	140±6	Competitive	160

t1.6 [MOI], multiplicity of infection.
t1.7 [a] Values determined by SPR.[24]

Please cite this article as: Farady, C. J. *et al.*, The Mechanism of Inhibition of Antibody-based Inhibitors of Membrane-type Serine Protease 1 (MT-SP1), *J. Mol. Biol.* (2007), doi:10.1016/j.jmb.2007.03.078

lecular substrates. From these data, approximate K_I values of 12 pM for E2 and 160 pM for S4 could be extrapolated (Table 1). Since the substrate (uPA) concentration could not be increased above K_M, the errors associated with K_I values are large; nonetheless, they confirm that the inhibitors inhibit MT-SP1 equally well, regardless of the size of the protease substrate.

Pre-steady-state kinetics

A closer examination of the progress curves of the steady-state reactions when enzyme was added to a mixture of substrate and inhibitor revealed different binding mechanisms for E2 and S4 (Figure 1). The progress curves for S4 are linear, suggesting the binding of scFv to enzyme comes to equilibrium rapidly. Conversely, the progress curves for E2 inhibition are curved, suggesting slow binding inhibition.[30] To define the binding mechanisms of these scFvs, stopped-flow experiments were performed to evaluate the onset of inhibition during turnover at higher concentrations of enzyme. Stopped-flow experiments measured the appearance of pNA, and were carried out as described in Materials and Methods.

The stopped-flow traces from the S4 inhibitor experiments were fit by nonlinear regression to the rate equations for reversible, tight-binding inhibition to obtain observed rate constants (k_{obs}) for the onset of inhibition (equation (5)).[31] Plots of k_{obs} *versus* [S4] are linear with positive *y*-intercepts (Figure 2(a)), consistent with a one-step reversible mechanism for binding the inhibitor. The *y*-intercepts of the plots give an average off-rate of $k_{-1} = 1.7 \times 10^{-2}$ s^{-1}, and a secondary plot of the slopes *versus* substrate concentration (Figure 2(a), inset) defined the on rate as $k_1 = 1.2 \times 10^8$ M^{-1}s^{-1}. The K_I calculated from $k_{-1}/k_1 = 147$ pM, which is in very good agreement with the steady-state K_I of 140 pM from experiment. From these data, it can be concluded that S4 binds and inhibits MT-SP1 with an extremely fast on-rate, and has a one-step binding mechanism as shown in Scheme 1.

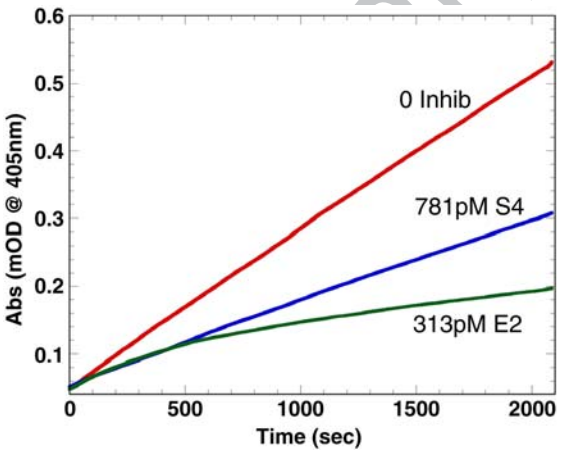

Figure 1. Progress curves of MT-SP1 inhibition by scFv inhibitors reveal multiple mechanisms of inhibition. The addition of 0.2 nM enzyme to a mixture of substrate (300 μM Spec-tPA) and inhibitor results in a decrease in proteolytic activity. S4 inhibition results in a linear progress curve, suggesting rapid-equilibrium inhibition, while the curved nature of the E2 progress curve suggests slow-binding inhibition.

Scheme 1.

The stopped-flow traces from the E2 inhibitor experiments (Figure 2(b)) revealed a more complicated binding mechanism. In this case, the progress curves fit well to a sum of two exponentials (equation (7)), indicating the presence of at least two steps in the binding process, which leads to the onset of inhibition. At minimum, a double-exponential decay is consistent with a two-step binding mechanism. This occurs when the first step in the binding process is more rapid than the second and, as a result, the first observed rate constant (k_{obs1}) shows a linear dependence on the concentration of inhibitor.[32] If k_{obs1} shows a hyperbolic dependence on inhibitor concentration, the mechanism of inhibition involves more than two steps. Unfortunately, due to the extremely tight nature of the enzyme–inhibitor interaction, the concentration of inhibitor could not be increased sufficiently to distinguish between a linear or hyperbolic dependence of k_{obs1} on the concentration of inhibitor. But, due to the presence of two exponential decays, an absolute minimal mechanism of E2 inhibition has two steps, and E2 can be classified as a slow, tight-binding inhibitor.[30]

p-Aminobenzamidine competition assay

p-Aminobenzamidine (pAB) has been reported as a weak competitive inhibitor of P1-arginine-specific serine proteases,[33] and can be used as a fluorescent probe to monitor substrate or inhibitor binding in the S1 site. The hydrophobic nature of the S1 site causes pAB to fluoresce with a maximum emission around 360 nm when bound to the enzyme, while pAB in aqueous solution has both a lower intensity and longer wavelength of emission at 376 nm. pAB has been used as a probe to monitor binding of inhibitors in the S1 site of inhibitors; competitive inhibitors displace pAB from the protease active site and reduce emission at 360 nm,[33,34] while non-competitive inhibitors do not.[35] pAB has a K_I of 28.8 μM for MT-SP1 (data not shown), and 1 μM MT-SP1 incubated with 270 μM PAB (to saturate the enzyme) shows a characteristic emission peak at 361 nm when excited at 325 nm (Figure 3). When one equivalent of either E2 or S4 is added to the pre-

Please cite this article as: Farady, C. J. *et al.*, The Mechanism of Inhibition of Antibody-based Inhibitors of Membrane-type Serine Protease 1 (MT-SP1), *J. Mol. Biol.* (2007), doi:10.1016/j.jmb.2007.03.078

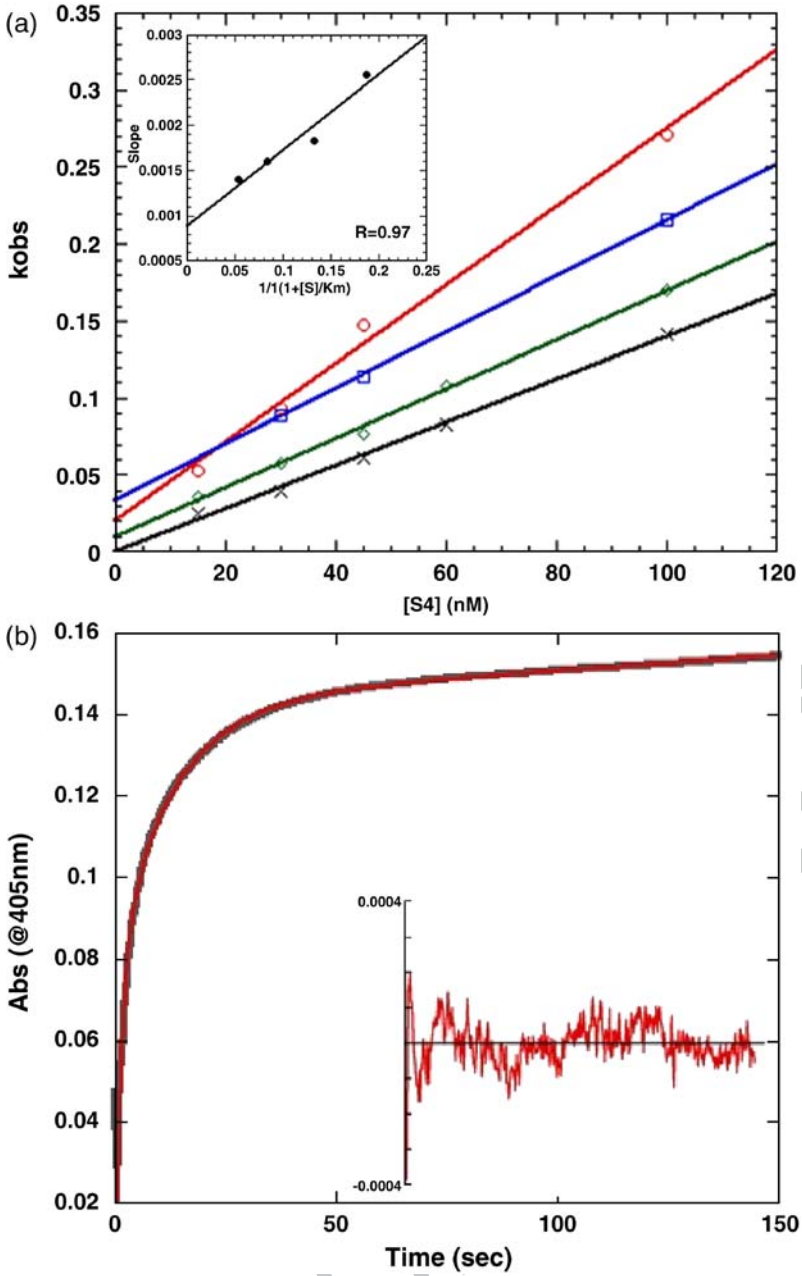

Figure 2. Stopped-flow experiments confirm disparate mechanisms of inhibitor binding to MT-SP1. (a) Linear plots of k_{obs} *versus* S4 concentration confirm that S4 has a one-step binding mechanism, as illustrated by Schem 1. Individual traces are for different concentrations substrate: black (×), 200 μM Spec-tPA; green (◇), 300 μM Spec-tPA; blue (□), 500 μM Spec-tPA; and red (○),800 μM Spec-tPA. (a) The *y*-intercepts of the observed rate constant plots gave an average off rate of $k_{-1} = 1.7 \times 10^{-2}\ s^{-1}$, and a secondary plot of the slopes *versus* concentration of substrate (inset) defined the on rate as $k_1 = 1.2 \times 10^8\ M^{-1}s^{-1}$. (b) The raw stopped-flow trace monitoring E2 inhibition of MT-SP1 by measuring the appearance of pNA at 405 nm fits well to the double exponential equation (7) with two observed rate constants. The inset shows the residuals of the non-linear regression fit. Final concentrations for this trace were 240 nM E2, 10 nM MT-SP1, and 500 μM Spec-tPA.

incubated MT-SP1/pAB, the fluorescence is decreased sharply (Figure 3). This suggests that both inhibitors bind at or near the S1 site, and most likely insert an arginine or lysine side-chain into the pocket.

MT-SP1/inhibitor digest

The reactive site of many standard mechanism serine protease inhibitors has been determined by incubating protease and inhibitor at low pH, where the inhibitor can be cleaved in a substrate-like manner, causing a processing of the inhibitor into two fragments, with the cleavage occurring between the P1 and P1′ residues.[36,37] When MT-SP1 and E2 are incubated at pH 6.0 for an extended period of time (>120 h), E2 is processed into two bands (Figure 4). This processing is not seen at pH 8.0, or without MT-SP1 at pH 6.0. MT-SP1 shows no proteolytic activity below pH 6.0, making this the lowest pH at which processing can occur. Electron spray ionization (ESI) mass spectrometry verifies that the processing event takes place between R131 and R132 in E2. The N-terminal fragment has a mass of 12,013 Da (expected 12,014 Da) and the C-terminal fragment has a mass of 15,624 Da (expected 15,627 Da). This places the reactive loop in the CDR3 of the heavy chain of E2, which would be expected from the HuCAL library from which these scFvs were matured, as the scaffold had large, diverse CDR3s.[29] No S4 processing was observed upon incubation with MT-SP1 for extended periods of time at low pH, suggesting a different, non-canonical mechanism of inhibition for the S4 scFv.

Please cite this article as: Farady, C. J. *et al.*, The Mechanism of Inhibition of Antibody-based Inhibitors of Membrane-type Serine Protease 1 (MT-SP1), *J. Mol. Biol.* (2007), doi:10.1016/j.jmb.2007.03.078

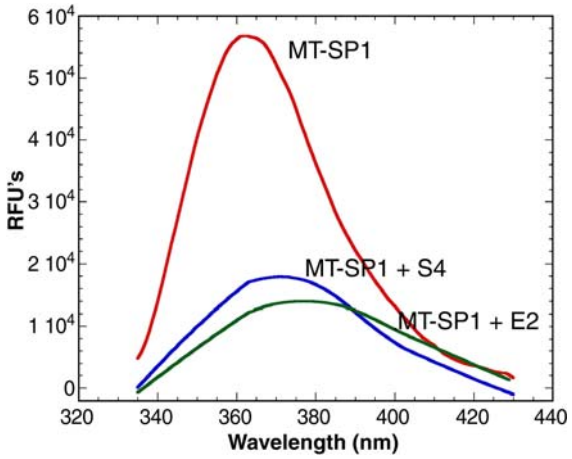

Figure 3. Inhibitors displace pAB from the MT-SP1 active site. pAB (270 μM) incubated with 1 μM MT-SP1 emits a strong emission peak with a maximum at 361 nm when excited at 325 nm, due to hydrophobic interactions between pAB and the P1 pocket of the protease. When one equivalent of either S4 (blue trace) or E2 (green trace) is added to 1 μM MT-SP1 saturated with pAB, the fluorescence decreases, suggesting pAB is released into the aqueous environment, where it is weakly fluorescent. Therefore, binding of both S4 and E2 are competitive with pAB binding, and both inhibitors bind in or near the P1 pocket in a manner that precludes binding of pAB.

Inhibitor point mutants

To verify the mechanism of inhibition of the scFv inhibitors, point mutants of the arginine residue in the CDR3 loops of the inhibitors were constructed. It would be expected that mutations to residues that bind in the S1 site of the protease would have the greatest effect on binding. The mutational data are summarized in Table 2. E2 R131A and R132A had K_I values of 78 nM and 454 pM, respectively (K_I = 12.3 pM for the wild-type E2). The mutation of R131 to alanine has a 6500-fold effect on protease inhibition, as would be expected from a residue that binds in the S1 site. This is consistent with the data from the inhibitor digest at low pH. The mutation of R132 caused a 38-fold increase in K_I, suggesting that the P1′ arginine also makes significant contacts with the protease. The CDR3 loop of S4 also has a double arginine motif, R128 and R129. Both arginine residues were mutated to alanine and had significant effects on protease inhibition: S4 R128A had a K_I of 2.8 μM, while the R129 alanine mutant had a K_I of 3.9 nM, a 4×10^4-fold and a 56-fold difference, respectively.

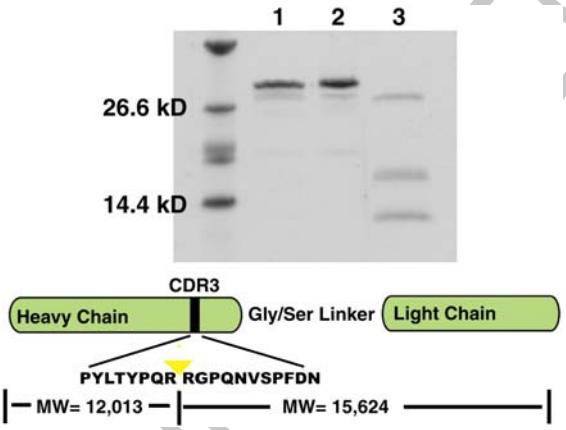

Figure 4. E2 is processed by MT-SP1 at pH 6.0. E2 (2 mM) was incubated at pH 6.0 with (lane 3) and without (lane 1) 0.1 μM MT-SP1 for 120 h. Samples were run on a 12% (w/v) polyacrylamide gel and stained with Coomassie brilliant blue. At pH 6.0, E2 was processed into two products, with molecular masses determined to be 15,624 Da, and 12,013 Da by ESI mass spectrometry. These masses, when added together, account for the mass of the full-length inhibitor (27,219 Da) and the water molecule added to the products during the hydrolysis reaction. This processing does not take place when E2 and MT-SP1 are incubated at pH 8.0 (lane2). The diagram below shows the site of the scissile bond in the middle of the heavy chain of E2.

MT-SP1 point mutations

To footprint the binding site of the inhibitors, site-directed mutagenesis was used to alanine scan the surface of the protease domain.[38] On the basis of the crystal structure of MT-SP1,[39] 30 point mutants were identified as potential partners in macromolecular interactions (Table 3). The majority of these residues were located on the loops flanking the protease active site. Proteolytic activity against Spec-tPA was used to assure that the point mutations did not drastically affect MT-SP1 structure or function. The differences between the mutant and wild-type protease k_{cat}/K_M values were less than twofold in most cases, suggesting that the mutations had minimal effect on protease structure. MT-SP1 T98A was a sixfold less efficient enzyme than the wild-type, which could be attributed primarily to a lower k_{cat}. MT-SP1 D217A had a threefold decrease in protease specific activity, which was due to an increased K_M of 210 μM. The F99A, Q192A, and W215A substitutions in MT-SP1 all resulted in inactive enzymes. The inactive variants eluted from a gel-filtration column at the same size as the zymogen protease, suggesting they are inactive because they could not autoactivate (data not shown).

The K_I values for E2 and S4 were determined against the MT-SP1 point mutants. As a positive control, the fold-specific serine protease inhibitor

Table 2. Inhibitor point mutant K_I *versus* MT-SP1

	K_I (nM)	Fold difference
E2	0.01	
E2 R131A	78	6500
E2 R132A	0.45	38
S4	0.07	
S4 R128A	2800	4.0×104
S4 R129A	3.9	56

All error values >6%.

Please cite this article as: Farady, C. J. *et al.*, The Mechanism of Inhibition of Antibody-based Inhibitors of Membrane-type Serine Protease 1 (MT-SP1), *J. Mol. Biol.* (2007), doi:10.1016/j.jmb.2007.03.078

t3.2 **Table 3.** MT-SP1 point mutant/inhibitor K_I values

t3.3		BPTI		E2		S4	
t3.4		K_I (pM)	Fold difference	K_I (pM)	Fold difference	K_I (pM)	Fold difference
t3.5	MT-SP1	49.7		12.3		70.4	
t3.6	Q38A	20.7	0.42	6.1	0.5	73.6	1
t3.7	I41A	12.4	***0.25 (fourfold)***	12.3	1	208	***3***
t3.8	I60A	35.8	0.72	50.4	***4.1***	40.2	0.57
t3.9	D60aA	37.2	0.75	25.1	2	125	1.8
t3.10	D60bA	628	***12.6***	20.8	1.7	427	***6.1***
t3.11	R60cA	134	2.7	11.4	0.93	11.7	***0.17 (sixfold)***
t3.12	F60eA	24.1	0.48	11.4	0.93	102	1.4
t3.13	R60fA	73.4	1.5	10.9	0.89	88.9	1.3
t3.14	Y60gA	43.5	0.88	12.7	1	151	2.1
t3.15	R87A	38.6	0.78	9.4	0.76	54.5	0.77
t3.16	F94A	170	***3.4***	36.2	2.9	1036	***15***
t3.17	N95A	83.6	1.7	45.4	***3.7***	108	1.5
t3.18	D96A	150	3	>1uM	***>105***	897	***13***
t3.19	F97A	224	***4.5***	>1uM	***>105***	154	2
t3.20	T98A	76.4	1.5	83.2	***6.7***	239	***3.4***
t3.21	H143A	48.5	1	14.2	1.2	1671	***24***
t3.22	Q145A	83.4	1.7	15.4	1.3	116	1.6
t3.23	Y146A	116	2.3	76.8	***6.2***	1405	***20***
t3.24	T150A	57.8	1.2	20.1	1.6	94.6	1.3
t3.25	L153A	116	2.3	21.7	1.8	116	1.6
t3.26	E169A	163	***3.3***	23.1	1.9	199	2.8
t3.27	Q174A	129	2.6	11.6	0.94	63.7	0.9
t3.28	Q175A	39.7	0.8	851	***69***	246	***3.5***
t3.29	D217A	2137	***43***	32	2.6	838	***12***
t3.30	Q221aA	63.4	1.3	40.5	***3.3***	65.7	0.93
t3.31	R222A	42.8	0.87	10.5	0.85	61.1	0.87
t3.32	K224A	111	2.2	46.3	***3.8***	59.1	0.84

t3.33 K_I is calculated from the IC_{50} value; all errors >6%.

BPTI was screened against the protease point mutants, since the mechanism of inhibition is known[40] and a the structure of a co-crystal of BPTI and MT-SP1 has been solved.[39] As would be expected from a fold-specific protease inhibitor, most point mutants had little effect on BPTI inhibition. The I41A substitution moderately improved BPTI binding to MT-SP1, F94A, F97A, and E169A moderately decreased BPTI inhibition (corresponding to <1 kcal/mol binding energy), and D60bA and D217A mutations had a more significant affect on BPTI inhibition (Figure 5(b)). Analysis of the crystal structure suggests that the increased K_I of MT-SP1 D60bA could be due to D60b hydrogen bonding with R20 of BPTI, and forming an intramolecular H-bond with R60c, which packs against BPTI. A deletion of the H-bonding ability of this side chain would account for the moderate increase (12.6-fold) in K_I. The structure does not readily explain the 43-fold increase in the K_I of BPTI for MT-SP1 D217A, but it is possible that the mutation affects the structure of the 220s loop, which would account also for the increased K_M of Spec-tPA for D217A.

On the basis of the alanine scanning data, S4 makes contacts of moderate strength with a number of residues on the six surface loops surrounding the active site (Figure 5(a) and (d)). Interactions with the side-chains of I41, D60b, T98, and Q175 account for modest binding energy (pink residues, Figure 5(d)); alanine mutations of these residues increased the K_I values of S4 3–6 fold, corresponding to a decrease in free energy of binding of 0.5–1 kcal/mol. S4 makes stronger interactions with the side-chains of F94, D96, H143, Y146, and D217 (red residues, Figure 5(d)), decreasing the free energy of binding by 1.5–2.0 kcal/mol. Interestingly, a mutation of R60c to alanine decreased the K_I of S4 6-fold. This suggests that the protease/scFv interaction has not been optimized completely. Taken together, the mutational data suggest that S4 makes a number of moderate contacts with the loops flanking the active site, making the strongest interactions with the 140s and 90s loops, and thereby bridging the active site.

E2 makes interactions with a number of loops surrounding the MT-SP1 active site (Figure 5(c)), including the base of the 60s loop, the 90s loop, the 170s loop, the 220s loop, and the 140s loop. In contrast to S4, which makes a number of interactions of moderate strength, E2 gains much of its binding energy from interactions with two residues, D96 and F97. Mutations of each of these residues to alanine increased the K_I of E2 to >1 μM, corresponding to a decrease in free energy of binding of >7.5 kcal/mol. The Q175A variant, on the loop adjacent to the 90s loop, also has a significant effect on E2 inhibition, increasing the K_I of E2 by 69-fold (3.0 kcal/mol). The 90s loop and 170s loop flank the extended binding sites of MT-SP1,[39,41] and F97 helps form the S4 pocket, suggesting E2 binds in the extended binding pockets of MT-SP1. Though E2 makes minor interactions with Y146, Q221a, and K224, the majority of the binding energy of E2 for MT-SP1 comes from interactions with the 90s loop, and minor interactions with residues flanking the 90s

Please cite this article as: Farady, C. J. *et al.*, The Mechanism of Inhibition of Antibody-based Inhibitors of Membrane-type Serine Protease 1 (MT-SP1), *J. Mol. Biol.* (2007), doi:10.1016/j.jmb.2007.03.078

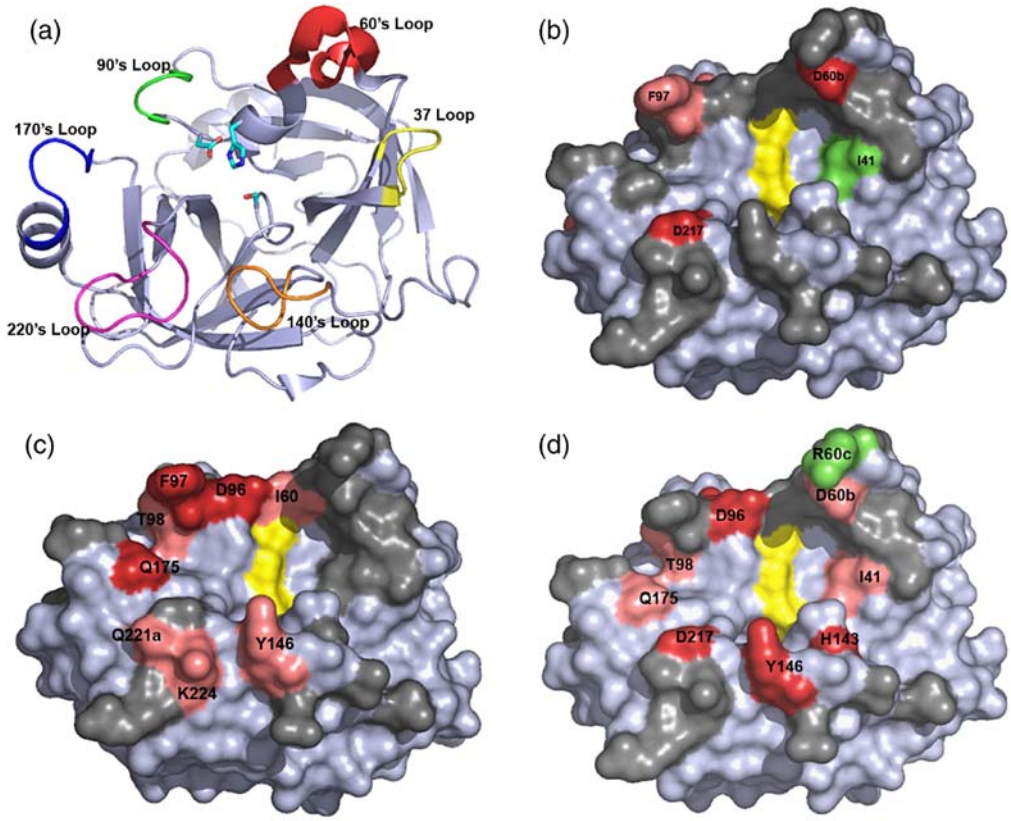

Figure 5. MT-SP1 alanine point mutants and their effect on protease inhibition by (b) BPTI, (c) E2, and (d) S4. (a) The 6 MT-SP1 surface loops surrounding the protease active site consisting of a binding cleft and the catalytic triad (sticks). The space-filling models shown in (b), (c), and (d) are oriented in the same manner, with the catalytic triad in yellow. Point mutants that had minimal effect on protease inhibition are shaded in gray, mutations that had a three-to tenfold increase in inhibitor K_I are shaded pink, and point mutants that increased inhibitor K_I by more than tenfold are shaded in red. Point mutants that decreased inhibitor K_I are shaded in green. The point-mutant/inhibitor K_I values are given in Table 3. MT-SP1 point mutants have a minimal effect on BPTI inhibition, S4 interacts with moderate affinity to all six protease loops surrounding the active site, and E2 binds with high affinity to the 90s and 170s loop. This Figure was prepared using PyMoL [http://www.pymol.sourceforge.net/].

loop (I60, Q175). This defines the 90s loop as a hot-spot for E2 binding; and as the 90s loop sequence is unique to MT-SP1, it helps explain E2s specificity for MT-SP1.

Discussion

We have described the mechanism by which two novel scFv antibodies inhibit the cancer-associated serine protease MT-SP1/matriptase. The S4 antibody has a fast association rate with MT-SP1 (1.2×10^8 $M^{-1}s^{-1}$ as measured by stopped-flow kinetics) and binds very tightly to the protease, making numerous contacts with the loops surrounding the active site of MT-SP1. The fast on-rate is likely influenced by electrostatic steering, which can increase k_{on} by more than 10^4 over the basal diffusion-controlled association rate.[42] Mutational data support this hypothesis, as nearly all the residues S4 makes significant contacts with are polar or charged. The inhibitor competes with pAB for the S1 site, and the R128A variant of S4 nearly abolishes protease inhibition. Despite these data, S4 cannot be considered a standard mechanism inhibitor of MT-SP1 without further structural characterization. Standard mechanism inhibitors have a characteristic two-step binding mechanism; an initial binding step, followed by a tightening of the enzyme–inhibitor complex and, as such, have an association rate approximately two orders of magnitude slower than S4. Furthermore, S4 is not processed by MT-SP1 at low pH, meaning the substrate-like binding cannot be assumed.

E2, on the other hand, displays all the characteristics of a standard mechanism serine protease inhibitor. While a crystal structure would help to determine the mechanism of inhibition definitively, the data here are consistent with E2 being a standard-mechanism inhibitor. The enzyme–inhibitor complex reaches equilibrium slowly, E2 binds in a substrate-like manner, and inserts an arginine residue into the S1 site of MT-SP1 (R131), which is important for, but not absolutely critical to, inhibition. Furthermore, E2 shows a slight degree of fold specificity; it inhibits the mouse homolog of MT-SP1, epithin, with a K_I of 40 nM,[24] and can inhibit trypsin, a digestive protease with extremely broad specifi-

Please cite this article as: Farady, C. J. *et al.*, The Mechanism of Inhibition of Antibody-based Inhibitors of Membrane-type Serine Protease 1 (MT-SP1), *J. Mol. Biol.* (2007), doi:10.1016/j.jmb.2007.03.078

city, with an IC_{50} of 45 μM (data not shown). In contrast to most standard mechanism serine protease inhibitors, E2 is highly specific for a single serine protease, MT-SP1. E2 gains much of its specificity through interactions with the 90s loop of MT-SP1, and makes significant interactions with residues D96 and F97 of the protease. Perhaps not surprisingly, known protease inhibitors that do exhibit a high degree of specificity, such as anticoagulant protease inhibitors from ticks and leeches, often employ a similar mechanism of inhibition; they combine the robustness of competitive, active site inhibition with protein extensions that bind to recognition sites on target enzymes.[5,43]

To our knowledge, these scFvs are the first documented case of mechanistic protease inhibitors on an antibody scaffold that bind in the active site. A number of monoclonal antibody protease inhibitors have been reported[17–19,21,22,44] but, despite diverse mechanisms, all have the same underlying mode of action; they bind to a small, linear peptide sequence and prevent either a protein–protein or an enzyme–substrate interaction. While often sufficient for inhibition, these monoclonal antibodies can have curious inhibitory profiles in which they cannot inhibit the hydrolysis of small-molecule substrates, or have different levels of inhibition against different substrates.[19,21] Because they are selected *in vitro* against the active form of the enzyme, antibodies developed by phage display have the inherent advantage of recognizing three-dimensional epitopes and the topography of the enzyme active site. With this comes the opportunity for tighter binding due to greater buried surface areas and minimal entropic penalties upon binding, and more complete inhibition through insertion of residues into the protease active site. E2 and S4 have clearly used these advantages; they have fast on-rates, very low K_D values, bind in the active site groove, and make contact with a number of loops flanking the active site.

The HuCAL-scFv library contains consensus framework sequences for all frequently occurring V_H and V_L subfamilies with a germline sequence for the CDR1 and CDR2 in each subfamily.[29] Both the heavy and light chain CDR3 regions were diversified according to the natural amino acid composition and cover the natural length variation of the V_H and V_L CDR3 regions. In retrospect, this proves to be an ideal scaffold for serine protease inhibition; it allows for a large, rigidified reactive loop to be inserted into the protease active site, while the rest of the antibody stabilizes the CDR3 of the heavy chain and makes additional contacts with the protease. While only the most potent scFv inhibitors of MT-SP1 were characterized, all inhibitors had heavy chain CDR3 loops of at least 17 residues, suggesting that large heavy chain CDR3s were critical to MT-SP1 inhibition.

The explosion in antibody research over the past 15 years has revolutionized biotechnology. Antibodies have been developed into extremely useful drugs and imaging devices, and have become critical tools in many areas of biological research. Here, scFv fragments have shown the ability to inhibit specifically a single member of a family of closely related enzymes. While these molecules will be useful in helping dissect the complex biology of MT-SP1,[45] the mechanisms through which they work once again reveals the innate binding flexibility of antibodies, and the power of protein engineering. That these inhibitors have developed the robust inhibition mechanism of standard mechanism serine protease inhibitors, suggests that we can develop antibodies to mimic any protein–protein interaction, and modulate nearly any biological process precisely.

Materials and Methods

Protein expression, purification, and mutagenesis

MT-SP1 and MT-SP1 mutants were expressed in *Escherichia coli* and purified from inclusion bodies as described.[25] Antibodies were selected from the HuCAL scFv library (MorphoSys AG, Martinsreid, Germany).[29] Expression and purification of inhibitory scFv antibodies were as described.[24] Point mutants were made using the Stratagene Quickchange kit (Stratagene, La Jolla, CA). One or two base changes were sufficient to create the point mutant in each case, and all sequences were verified by DNA sequencing.

Steady-state kinetics

All reaction volumes were 120 μl and were carried out in 50 mM Tris–HCl (pH 8.8), 50 mM NaCl, 0.01% (v/v) Tween-20 unless stated otherwise and all reactions were carried out in triplicate. Reactions were run in 96-well, medium-binding, flat-bottomed plates (Corning), and cleavage of substrate was measured with a UVmax Microplate Reader (Molecular Devices Corporation, Palo Alto, CA.). MT-SP1 and mutant protease concentrations were determined by 4-methylumbelliferyl *p*-guanidinobenzoate active-site titration with a Fluormax-2 spectrofluorimeter.[46] Kinetic parameters of MT-SP1 and mutant proteases were determined at 0.2 nM enzyme, with concentrations of Spectrazyme-tPA (hexahydrotyrosyl-Gly-Arg-pNA, American Diagnostica, Greenwich, CT) varying from 1 μM to 400 μM. K_M and k_{cat} were determined using the Michaelis–Menten equation.

Tight-binding inhibitors require that the effective decrease in free enzyme be taken into account when determining K_I values.[31] This is accomplished by incubating enzyme and inhibitor so that the system can reach equilibrium, adding substrate, and then measuring steady-state velocities at various concentrations of inhibitor and fitting the data to:

$$v_i/v_s = \left\{ \frac{[E_T - I_T - K_i^*] + [(I_T + K_i^* - E_T)^2 + (4K_i^* E_T)]^{1/2}}{2E_T} \right\} \quad (1)$$

K_I^* values are then plotted against substrate concentration to extrapolate the K_I at zero substrate concentration:

$$K_i^* = K_i(1 + [S]/K_m) \quad (2)$$

Please cite this article as: Farady, C. J. *et al.*, The Mechanism of Inhibition of Antibody-based Inhibitors of Membrane-type Serine Protease 1 (MT-SP1), *J. Mol. Biol.* (2007), doi:10.1016/j.jmb.2007.03.078

When measuring the effect mutations had on the strength of the interaction between the protease and inhibitor, IC_{50} values were used instead of K_I' as determined above. Though less accurate than K_I,[47] IC_{50} is easier to calculate when screening large numbers of inhibitor point mutants, and is sufficient to monitor relative changes in inhibition *versus* the wild-type system. IC_{50} was determined by incubating inhibitor and 0.2 nM enzyme for at least 5 h at room temperature to assure steady-state behavior of the system.[3] There was no appreciable decrease in protease activity during the incubation period. Steady-state velocities were then plotted against inhibitor concentration and fit to:

$$v = v_{min} + \frac{(v_{max} - v_{min})}{(1 + 10^{([I]-IC_{50})})} \quad (3)$$

Relative K_I' was calculated from IC_{50} values according to:

$$K_I = \frac{IC_{50}}{(1 + [S]/K_M)} \quad (4)$$

Though nearly all protease mutants had a minimal (less than twofold) effect on substrate K_M, and the substrate concentration was held well above the K_M, this correction normalizes the IC_{50} with respect to the strength of the protease/substrate interaction. All graphs and equations were fit using Kaliedagraph 3.6 (Synergy Software, Reading, PA).

Macromolecular substrate assay

In an assay analogous to that used to monitor factor VIIa activation of FX,[8] we developed a coupled assay that monitors MT-SP1 activation of uPA in which 50 pM MT-SP1 was incubated with various concentrations (final concentrations, 12.5–400 nM) of single-chain uPA (American Diagnostica). At various time-points (0–150 min), aliquots of the reaction were removed and quenched with 10 nM E2. There was no residual MT-SP1 activity after the quench, and E2 showed no inhibition of uPA at a concentration of 10 nM. The amount of active uPA was measured by monitoring the activity for uPA against the *para*-nitroanilide uPA substrate Spectrazyme-UK (American Diagnostica). The mode of inhibition was determined from double reciprocal plots, and kinetic parameters and inhibition constants were determined using the Michaelis–Menten equation. The K_M of Spec-UK for uPA was determined to be 42 μM, and the k_{cat} of uPA turnover was 1.0 s^{-1}.

Stopped-flow kinetics

Stopped-flow experiments were conducted using a HiTech SF-61DX2 instrument (TgK Scientific Ltd., Bradford on Avon, U.K.). Data were collected in dual beam mode using photomultiplier detection of absorbance data at 405 nm. MT-SP1 (10 nM for E2 experiments, 1 nM for S4 experiments) was mixed rapidly with a solution of substrate (Spec-tPA, 200–800 μM) and inhibitor (10–300 nM for S4, 100–340 nM for E2) and the appearance of pNA was monitored for 20 s (for S4) or 150 s (for E2). Concentrations of enzyme and length of experiments were varied between the two systems to ensure robust signal and equilibration of the system.

The stopped-flow traces from the S4 inhibitor experiments were fit by nonlinear regression to the rate equations for reversible, tight binding inhibition:[31]

$$P = v_s t + (v_i - v_s)(1 - e^{-k_{obs}t})/k_{obs} \quad (5)$$

The appearance of the product (P) is a function of the initial (v_i) and final (v_s) velocities, and an apparent first-order rate constant, k_{obs} for the onset of inhibition. Plots of k_{obs} *versus* inhibitor concentration were linear, and fit to equation (6), as would be expected when the inhibitory mechanism consists of one reversible binding step, as in Scheme 1:

$$k_{obs} = k_{-1} + k_1[I]/(1 + [S]/K_M) \quad (6)$$

E2 stopped-flow traces fit poorly to equation (5), but fit well to a mechanism with two observed rate constants:[32]

$$P = v_s t + (v_i - v_s)(1 - e^{-k_{obs1}t})/k_{obs1} + (v_i - v_s)(1 - e^{-k_{obs2}t})/k_{obs2} \quad (7)$$

p-Aminobenzamidine fluorescence

Experiments were carried out in PBS with a Fluorolog 3 (Instruments SA Inc. Edison, NJ) fluorimeter. Emission spectra of MT-SP1/pAB were obtained by excitation at 325 nm using a 4 nm excitation and 2 nm emission bandpass, and were scanned from 335–430 nm. Spectra were corrected for emission due to free pAB and protease. Data corrections were performed with Datamax 2.20 software (Instruments SA).

Inhibitor digest

E2 (2 μM) or S4 (2 μM) was incubated with 0.1 nM MT-SP1 for 120 h at room temperature. Proteins were incubated in 100 mM Mes (pH 6.0), 100 mM NaCl or in 50 mM Tris–HCl (pH 8.0), 100 mM NaCl. Proteolysis was monitored by gel mobility-shift on a 12% (w/v) polyacrylamide gel with a 4.5% stacking gel, and stained with Coomassie brilliant blue. ESI mass spectrometry was carried out with an LCT Premier mass spectrometer (Waters Corp. Milford, MA), and molecular masses were determined using MassLynx (Waters) deconvolution software.

Acknowledgements

We thank Jill Winter (Chiron) and MorphoSys, AG for access to the HuCAL-scFv libraries, and Dr Ami Bhatt, Dr Alan Marnett, and Dr Sami Mahrus for many helpful discussions. This work was funded by a Program Project Grant for proteases in cancer, NIH CA72006 (to C.S.C.), the Department of Defense Breast Cancer Research Program BC043431 (C.J.F.) and NIH training grant GM08284 (M.R.D.). HuCAL is a registered trademark of MorphoSys, AG.

Please cite this article as: Farady, C. J. *et al.*, The Mechanism of Inhibition of Antibody-based Inhibitors of Membrane-type Serine Protease 1 (MT-SP1), *J. Mol. Biol.* (2007), doi:10.1016/j.jmb.2007.03.078

References

1. Rawlings, N. D., Morton, F. R. & Barrett, A. J. (2006). MEROPS: the peptidase database. *Nucl. Acids Res.* **34**, D270–D272.
2. Laskowski, M., Jr & Kato, I. (1980). Protein inhibitors of proteinases. *Annu. Rev. Biochem.* **49**, 593–626.
3. Eggers, C. T., Wang, S. X., Fletterick, R. J. & Craik, C. S. (2001). The role of ecotin dimerization in protease inhibition. *J. Mol. Biol.* **308**, 975–991.
4. Tyndall, J. D., Nall, T. & Fairlie, D. P. (2005). Proteases universally recognize beta strands in their active sites. *Chem. Rev.* **105**, 973–999.
5. Rydel, T. J., Tulinsky, A., Bode, W. & Huber, R. (1991). Refined structure of the hirudin-thrombin complex. *J. Mol. Biol.* **221**, 583–601.
6. Castro, M. J. & Anderson, S. (1996). Alanine point-mutations in the reactive region of bovine pancreatic trypsin inhibitor: effects on the kinetics and thermodynamics of binding to beta-trypsin and alpha-chymotrypsin. *Biochemistry*, **35**, 11435–11446.
7. Coussens, L. M., Fingleton, B. & Matrisian, L. M. (2002). Matrix metalloproteinase inhibitors and cancer: trials and tribulations. *Science*, **295**, 2387–2392.
8. Dennis, M. S., Eigenbrot, C., Skelton, N. J., Ultsch, M. H., Santell, L., Dwyer, M. A. *et al.* (2000). Peptide exosite inhibitors of factor VIIa as anticoagulants. *Nature*, **404**, 465–470.
9. Roberge, M., Santell, L., Dennis, M. S., Eigenbrot, C., Dwyer, M. A. & Lazarus, R. A. (2001). A novel exosite on coagulation factor VIIa and its molecular interactions with a new class of peptide inhibitors. *Biochemistry*, **40**, 9522–9531.
10. Krook, M., Lindbladh, C., Eriksen, J. A. & Mosbach, K. (1997). Selection of a cyclic nonapeptide inhibitor to alpha-chymotrypsin using a phage display peptide library. *Mol. Divers.* **3**, 149–159.
11. Hansen, M., Wind, T., Blouse, G. E., Christensen, A., Petersen, H. H., Kjelgaard, S. *et al.* (2005). A urokinase-type plasminogen activator-inhibiting cyclic peptide with an unusual P2 residue and an extended protease binding surface demonstrates new modalities for enzyme inhibition. *J. Biol. Chem.* **280**, 38424–38437.
12. Wang, C. I., Yang, Q. & Craik, C. S. (1995). Isolation of a high affinity inhibitor of urokinase-type plasminogen activator by phage display of ecotin. *J. Biol. Chem.* **270**, 12250–12256.
13. Dennis, M. S. & Lazarus, R. A. (1994). Kunitz domain inhibitors of tissue factor-factor VIIa. II. Potent and specific inhibitors by competitive phage selection. *J. Biol. Chem.* **269**, 22137–22144.
14. Stoop, A. A. & Craik, C. S. (2003). Engineering of a macromolecular scaffold to develop specific protease inhibitors. *Nature Biotechnol.* **21**, 1063–1068.
15. Binz, H. K., Amstutz, P., Kohl, A., Stumpp, M. T., Briand, C., Forrer, P. *et al.* (2004). High-affinity binders selected from designed ankyrin repeat protein libraries. *Nature Biotechnol.* **22**, 575–582.
16. Rezacova, P., Lescar, J., Brynda, J., Fabry, M., Horejsi, M., Sedlacek, J. & Bentley, G. A. (2001). Structural basis of HIV-1 and HIV-2 protease inhibition by a monoclonal antibody. *Structure*, **9**, 887–895.
17. Puchi, M., Quinones, K., Concha, C., Iribarren, C., Bustos, P., Morin, V. *et al.* (2006). Microinjection of an antibody against the cysteine-protease involved in male chromatin remodeling blocks the development of sea urchin embryos at the initial cell cycle. *J. Cell Biochem.* **98**, 335–342.
18. Fukuoka, Y. & Schwartz, L. B. (2006). The B12 anti-tryptase monoclonal antibody disrupts the tetrameric structure of heparin-stabilized beta-tryptase to form monomers that are inactive at neutral pH and active at acidic pH. *J. Immunol.* **176**, 3165–3172.
19. Petersen, H. H., Hansen, M., Schousboe, S. L. & Andreasen, P. A. (2001). Localization of epitopes for monoclonal antibodies to urokinase-type plasminogen activator: relationship between epitope localization and effects of antibodies on molecular interactions of the enzyme. *Eur. J. Biochem.* **268**, 4430–4439.
20. Matias-Roman, S., Galvez, B. G., Genis, L., Yanez-Mo, M., de la Rosa, G., Sanchez-Mateos, P. *et al.* (2005). Membrane type 1-matrix metalloproteinase is involved in migration of human monocytes and is regulated through their interaction with fibronectin or endothelium. *Blood*, **105**, 3956–3964.
21. Xuan, J. A., Schneider, D., Toy, P., Lin, R., Newton, A., Zhu, Y. *et al.* (2006). Antibodies neutralizing hepsin protease activity do not impact cell growth but inhibit invasion of prostate and ovarian tumor cells in culture. *Cancer Res.* **66**, 3611–3619.
22. Obermajer, N., Premzl, A., Zavasnik Bergant, T., Turk, B. & Kos, J. (2006). Carboxypeptidase cathepsin X mediates beta2-integrin-dependent adhesion of differentiated U-937 cells. *Expt. Cell Res.* **312**, 2515–2527.
23. Maun, H. R., Eigenbrot, C. & Lazarus, R. A. (2003). Engineering exosite peptides for complete inhibition of factor VIIa using a protease switch with substrate phage. *J. Biol. Chem.* **278**, 21823–21830.
24. Sun, J., Pons, J. & Craik, C. S. (2003). Potent and selective inhibition of membrane-type serine protease 1 by human single-chain antibodies. *Biochemistry*, **42**, 892–900.
25. Takeuchi, T., Shuman, M. A. & Craik, C. S. (1999). Reverse biochemistry: use of macromolecular protease inhibitors to dissect complex biological processes and identify a membrane-type serine protease in epithelial cancer and normal tissue. *Proc. Natl Acad. Sci. USA*, **96**, 11054–110561.
26. Lin, C. Y., Anders, J., Johnson, M. & Dickson, R. B. (1999). Purification and characterization of a complex containing matriptase and a Kunitz-type serine protease inhibitor from human milk. *J. Biol. Chem.* **274**, 18237–18242.
27. Uhland, K. (2006). Matriptase and its putative role in cancer. *Cell Mol. Life Sci.* **63**, 2968–2978.
28. List, K., Szabo, R., Molinolo, A., Sriuranpong, V., Redeye, V., Murdock, T. *et al.* (2005). Deregulated matriptase causes ras-independent multistage carcinogenesis and promotes ras-mediated malignant transformation. *Genes Dev.* **19**, 1934–1950.
29. Knappik, A., Ge, L., Honegger, A., Pack, P., Fischer, M., Wellnhofer, G. *et al.* (2000). Fully synthetic human combinatorial antibody libraries (HuCAL) based on modular consensus frameworks and CDRs randomized with trinucleotides. *J. Mol. Biol.* **296**, 57–86.
30. Morrison, J. F. & Walsh, C. T. (1988). The behavior and significance of slow-binding enzyme inhibitors. *Advan. Enzymol. Relat. Areas Mol. Biol.* **61**, 201–301.
31. Williams, J. W. & Morrison, J. F. (1979). The kinetics of reversible tight-binding inhibition. *Methods Enzymol.* **63**, 437–467.
32. Hiromi, K. (1979). *Kinetics of Fast Enzyme Reaction: Theory and Pratice.* Kodansha Ltd., Wiley, Tokyo.
33. Evans, S. A., Olson, S. T. & Shore, J. D. (1982). *p*-Aminobenzamidine as a fluorescent probe for the active site of serine proteases. *J. Biol. Chem.* **257**, 3014–3017.
34. Parry, M. A., Maraganore, J. M. & Stone, S. R. (1994).

Please cite this article as: Farady, C. J. *et al.*, The Mechanism of Inhibition of Antibody-based Inhibitors of Membrane-type Serine Protease 1 (MT-SP1), *J. Mol. Biol.* (2007), doi:10.1016/j.jmb.2007.03.078

Kinetic mechanism for the interaction of Hirulog with thrombin. *Biochemistry*, **33**, 14807–14814.
35. Fernandez, A. Z., Tablante, A., Beguin, S., Hemker, H. C. & Apitz-Castro, R. (1999). Draculin, the anticoagulant factor in vampire bat saliva, is a tight-binding, noncompetitive inhibitor of activated factor X. *Biochim. Biophys. Acta*, **1434**, 135–142.
36. Ozawa, K. & Laskowski, M., Jr (1966). The reactive site of trypsin inhibitors. *J. Biol. Chem.* **241**, 3955–3961.
37. McGrath, M. E., Hines, W. M., Sakanari, J. A., Fletterick, R. J. & Craik, C. S. (1991). The sequence and reactive site of ecotin. A general inhibitor of pancreatic serine proteases from *Escherichia coli*. *J. Biol. Chem.* **266**, 6620–6625.
38. Cunningham, B. C. & Wells, J. A. (1989). High-resolution epitope mapping of hGH-receptor interactions by alanine-scanning mutagenesis. *Science*, **244**, 1081–1085.
39. Friedrich, R., Fuentes-Prior, P., Ong, E., Coombs, G., Hunter, M., Oehler, R. *et al.* (2002). Catalytic domain structures of MT-SP1/matriptase, a matrix-degrading transmembrane serine proteinase. *J. Biol. Chem.* **277**, 2160–2168.
40. Luthy, J. A., Praissman, M., Finkenstadt, W. R. & Laskowski, M., Jr (1973). Detailed mechanism of interaction of bovine-trypsin with soybean trypsin inhibitor (Kunitz). I. Stopped flow measurements. *J. Biol. Chem.* **248**, 1760–1771.
41. Sriprapundh, D., Craik, C. S. (2006).
42. Schreiber, G. & Fersht, A. R. (1996). Rapid, electrostatically assisted association of proteins. *Nature Struct. Biol.* **3**, 427–431.
43. Rezaie, A. R. (2004). Kinetics of factor Xa inhibition by recombinant tick anticoagulant peptide: both active site and exosite interactions are required for a slow- and tight-binding inhibition mechanism. *Biochemistry*, **43**, 3368–3375.
44. Martin, F., Volpari, C., Steinkuhler, C., Dimasi, N., Brunetti, M., Biasiol, G. *et al.* (1997). Affinity selection of a camelized V(H) domain antibody inhibitor of hepatitis C virus NS3 protease. *Protein Eng.* **10**, 607–614.
45. Bhatt, A. S., Welm, A., Farady, C. J., Vasquez, M., Wilson, K. & Craik, C. S. (2007). Coordinate expression and functional profiling identify and extracellular proteolytic signaling pathway. *Proc. Natl Acad. Sci. USA.*
46. Jameson, G. W., Roberts, D. V., Adams, R. W., Kyle, W. S. & Elmore, D. T. (1973). Determination of the operational molarity of solutions of bovine alpha-chymotrypsin, trypsin, thrombin and factor Xa by spectrofluorimetric titration. *Biochem. J.* **131**, 107–117.
47. Chou, T. (1974). Relationships between inhibition constants and fractional inhibition in enzyme-catalyzed reactions with different numbers of reactants, different reaction mechanisms, and different types and mechanisms of inhibition. *Mol. Pharmacol.* **10**, 235–247.

Edited by I. Wilson

(Received 23 February 2007; accepted 20 March 2007)

Please cite this article as: Farady, C. J. *et al.*, The Mechanism of Inhibition of Antibody-based Inhibitors of Membrane-type Serine Protease 1 (MT-SP1), *J. Mol. Biol.* (2007), doi:10.1016/j.jmb.2007.03.078

PNAS
Proceedings of the National Academy of Sciences of the United States of America www.pnas.org

Coordinate expression and functional profiling identify an extracellular proteolytic signaling pathway

Ami S. Bhatt, Alana Welm, Christopher J. Farady, Maximiliano Vásquez, Keith Wilson, and Charles S. Craik

PNAS published online Mar 27, 2007;
doi:10.1073/pnas.0606514104

Coordinate expression and functional profiling identify an extracellular proteolytic signaling pathway

Ami S. Bhatt*, Alana Welm[†‡], Christopher J. Farady*, Maximiliano Vásquez[§], Keith Wilson[§], and Charles S. Craik*[¶]

*Department of Pharmaceutical Chemistry, University of California, 600 16th Street, San Francisco, CA 94158; [†]The G. W. Hooper Foundation, University of California, 513 Parnassus Avenue, San Francisco, CA 94153; and [§]PDL Biopharma, Inc., 34801 Campus Drive, Fremont, CA 94555

Edited by James A. Wells, University of California, San Francisco, CA, and approved February 6, 2007 (received for review July 30, 2006)

A multidisciplinary method combining transcriptional data, specificity profiling, and biological characterization of an enzyme may be used to predict novel substrates. By integrating protease substrate profiling with microarray gene coexpression data from nearly 2,000 human normal and cancerous tissue samples, three fundamental components of a protease-activated signaling pathway were identified. We find that MT-SP1 mediates extracellular signaling by regulating the local activation of the prometastatic growth factor MSP-1. We demonstrate MT-SP1 expression in peritoneal macrophages, and biochemical methods confirm the ability of MT-SP1 to cleave and activate pro-MSP-1 *in vitro* and in a cellular context. MT-SP1 induced the ability of MSP-1 to inhibit nitric oxide production in bone marrow macrophages. Addition of HAI-1 or an MT-SP1-specific antibody inhibitor blocked the proteolytic activation of MSP-1 at the cell surface of peritoneal macrophages. Taken together, our work indicates that MT-SP1 is sufficient for MSP-1 activation and that MT-SP1, MSP-1, and the previously shown MSP-1 tyrosine kinase receptor RON are required for peritoneal macrophage activation. This work shows that this triad of growth factor, growth factor activator protease, and growth factor receptor is a protease-activated signaling pathway. Individually, MT-SP1 and RON overexpression have been implicated in cancer progression and metastasis. Transcriptional coexpression of these genes suggests that this signaling pathway may be involved in several human cancers.

cancer | macrophage activation | protease substrate specificity | proteomics

Despite the successful physiological and biochemical characterization of many proteases, the vast majority of the >2% of the human genome that encodes proteases has yet to be functionally classified. Although many approaches demonstrate the sufficiency of a protease to cleave a given substrate, very few are able to address the physiological relevance of such *in vitro* findings. Cell-surface proteolysis is suggested to play a major role in cancer progression and metastasis through the processing of macromolecules important for regulating the extracellular environment. The cell-surface localization, high activity, and exquisite specificity of type II transmembrane serine proteases (TTSPs) suggest a role in outside-in signaling and interaction with the microenvironment. We elected to apply a multifaceted approach to identify physiologically relevant substrates of one prominent member of this family, membrane type serine protease 1 (MT-SP1/matriptase).

Members of the TTSP family, such as hepsin and MT-SP1, are highly expressed in many cancers, including those of the prostate, breast, colon, and ovary (1–9). Both overexpression and inhibition studies have supported the role of MT-SP1 in tumorigenesis and tumor growth. Targeted overexpression of MT-SP1 in squamous epithelia in mice results in skin-limited nodules of squamous cell carcinoma that become metastatic in the presence of the chemical carcinogen DMBA (10). Small molecule and macromolecular inhibitors of MT-SP1 have been developed and applied in a mouse model of cancer, resulting in growth suppression of androgen-independent prostate cancer xenografts (2, 11). Taken together, these findings suggest a role for MT-SP1 in cancer.

In this study, we sought to explore the mechanism of MT-SP1's activity in more detail. Although transcriptional coregulation has been reported between known pathway components, it has not been applied for the prediction of novel enzyme substrates (12, 13). Transcriptional profiling of nearly 2,000 human samples, including those from normal tissues, cancer cell lines, and 17 types of cancer tissue was performed to determine expression levels of MT-SP1, its candidate substrates, and its proposed endogenous inhibitor, the hepatocyte growth factor activator 1 (HAI-1) (14). Candidate substrates whose expression correlated with that of MT-SP1 in a statistically significant fashion were chosen for subsequent biochemical validation. These substrates were tested and validated in primary cells. Using this approach, we identified the cancer-associated growth factor macrophage-stimulating protein 1 (MSP-1) as a substrate of MT-SP1.

Results

Use of PS-SCL and Other Specificity Data to Guide Candidate Substrate Selection. Limited information on MT-SP1 substrate specificity was collected by using a complete diverse positionally scanned synthetic combinatorial library (PS-SCL) of synthetic substrates. The method can be used to identify consensus, nonprime side cleavage motifs for proteases (15). Our functional characterization of the binding specificity of MT-SP1 at the substrate-binding cleft is in accord with the information obtained from structural studies revealing trypsin-like specificity at the S1 position, a shallow pocket for small, hydrophobic residues at the S2 position, and an open negatively charged cavity at the S4 position, allowing for binding of a basic residue at P3 or P4 (16). Given the relative degeneracy of the specificity information obtained through biochemical profiling and structural studies, additional information was considered in the development of a consensus cleavage sequence. By using the specificity determinants obtained from the PS-SCL data and an alignment of known macromolecular substrates, a set of consensus sequences for MT-SP1 cleavage was deduced. The specificity of MT-SP1 was in fairly good agreement with the described cleavage sequence of the HGF-homolog, MSP-1 (Table 1).

Author contributions: A.S.B. and C.S.C. designed research; A.S.B. and A.W. performed research; A.S.B., A.W., C.J.F., M.V., and K.W. contributed new reagents/analytic tools; A.S.B., A.W., and C.S.C. analyzed data; and A.S.B. and C.S.C. wrote the paper.

The authors declare no conflict of interest.

This article is a PNAS Direct Submission.

Freely available online through the PNAS open access option.

Abbreviations: MT-SP1, membrane type serine protease 1; MSP-1, macrophage stimulating protein 1; HAI-1, hepatocyte growth factor activator inhibitor 1; TTSP, type two transmembrane serine protease; PS-SCL, positional scanning synthetic combinatorial library.

[‡]Present address: Department of Oncological Sciences, Huntsman Cancer Institute, University of Utah, Salt Lake City, UT 84112.

[¶]To whom correspondence should be addressed at: University of California, Genentech Hall, 600 16th Street, San Francisco, CA 94158-2517. E-mail: craik@cgl.ucsf.edu.

This article contains supporting information online at www.pnas.org/cgi/content/full/0606514104/DC1.

BIOCHEMISTRY

Table 1. Alignment of MSP-1 activation sequence with the predicted MT-SP1 cleavage sequence consensus

	P4	P3	P2	P1
Filaggrin	R	K	R	R
HGF/SF	K	Q	L	R
MT-SP1/matriptase	R	Q	A	R
PAR2	S	K	G	R
Trask/CDCP1/SIMA135	K	Q	S	R
uPA/urokinase	P	R	F	K
*P1-diverse PS-SCL	K/R	K/R	S > P > G > L	K/R
Phage Display	K/R vs. X	X vs. K/R	Small/hydrophobic	K/R
Crystal Structure	K/R vs. X	X vs. K/R	Small/hydrophobic	K/R
Consensus	K/R vs. S/P	Q vs. K/R	Small/hydrophobic	R > K
*MSP-1	S	K	L	R

Per standard notation, P1 is designated as the amino acid N-terminal to the scissile bond with P2 being the amino acid N-terminal to P1, etc. The P4 through P1 amino acids for known substrates of MT-SP1, P1-diverse PS-SCL data, phage display data, and crystallographic determinations are displayed. An MT-SP1 consensus cleavage sequence was derived from this information. The MSP-1 activation sequence is also presented. Asterisks indicate compiled PS-SCL data or MT-SP1 cleavage sequences determined by N-terminal sequencing in this work.

Transcriptional Profiling of Candidate MT-SP1 Substrates Demonstrates Two Candidate Proteins That Are Coexpressed with MT-SP1. To measure candidate gene RNA levels in human tissues and cell lines, tumor samples and cancer-derived cell lines were obtained from multiple sources. Tumor samples were obtained from the following tissue types: bladder, breast, cervical, colon, esophageal, head and neck, lung, ovarian, pancreatic, prostate, renal, stomach, testicular, and uterine cancers as well as Ewing's sarcoma, glioblastoma, and melanoma. Fifty-nine cancer cell lines, largely obtained from the American Type Culture Collection (Manassas, VA), were cultured *in vitro* and as SCID mouse xenografts. RNA was extracted from these samples, and RNA from 382 samples representing 86 types of nonpathogenic tissue was obtained from commercial sources. A single, custom microarray chip was designed to contain 400,000 perfect-match probes (≈59,000 probe sets). These arrays were then probed with biotinylated cDNA derived from the sample RNAs, and binding was quantitated by fluorescence. Genes of interest, such as described and predicted MT-SP1 substrates, the hepatocyte growth factor activator inhibitor 1 (HAI-1), and common cancer markers were chosen for further analysis. Both Pearson's product moment correlation coefficients and Spearman's rank-order correlation coefficients were calculated for all the given genes paired with MT-SP1. Bonferroni-corrected P values and false discovery rate P values are presented in supporting information (SI) Table 2. The data are summarized in Fig. 1, with statistical significance of the correlation established as $P < 0.05$ after Bonferroni correction or the false discovery rate correction (see *Methods* and *SI Appendix*). Significant correlations were not detected in cervical cancer, esophageal cancer, fetal tissues, head and neck cancer, Ewing's sarcoma, renal cancer, melanoma, or testicular cancer.

Expression of HAI-1 and MT-SP1 was significantly correlated in 13 of the tissue/cell line categories studied. The range of unadjusted P values calculated for the Pearson's product moment correlation coefficient range from 1.83×10^{-45} (HAI-1; normal tissues) to 0.994. The range of unadjusted P values calculated for the Spearman's rank-order correlation coefficient range from 5.85×10^{-34} (HAI-1; normal tissues) to 1. The most highly significant correlation detected was between HAI-1 and MT-SP1 in the aggregated sample of individually characterized normal body tissues.

This analysis showed that the expression of MT-SP1 and two of its previously described substrates, Trask and PAR2, was also significantly correlated in many tissue types. Interestingly, expression of the described MT-SP1 substrate HGF did not correlate well with MT-SP1 expression at the transcriptional level. Transcriptional expression of the HGF homolog, MSP-1, however, correlated well with expression of the protease in normal tissues and in certain cancers (Fig. 1). Furthermore, expression of the receptor for MSP-1, RON, very strongly correlated with MT-SP1 expression. Although RON has a fairly narrow expression pattern in normal tissues, including terminally differentiated macrophages, keratinocytes, several types of columnar epithelium, and osteoclasts (17), our data demonstrated aberrant receptor expression in certain cancer tissues. MT-SP1 and RON transcript levels were correlated in several tissue types

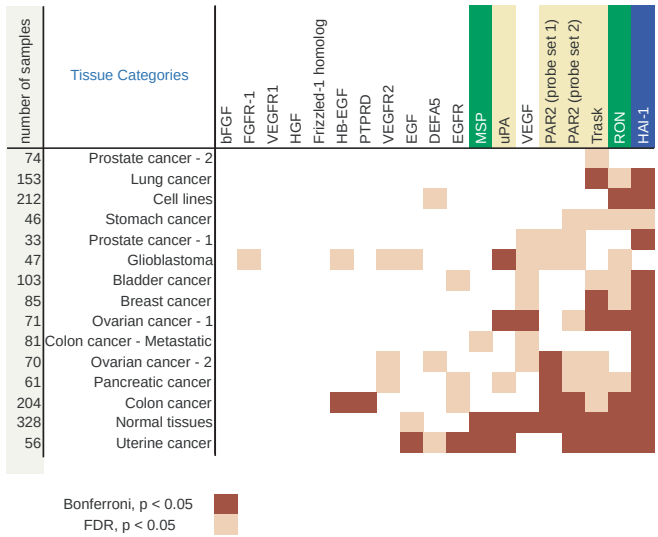

Fig. 1. Correlational cluster diagram of MT-SP1 and associated proteins. Transcriptional profiling of 19 genes was performed for nearly 2,000 samples from cell lines, normal tissues, and cancer tissues. Pearson's and Spearman's correlation coefficients were calculated for each gene paired with MT-SP1. Associated P values were also calculated and corrected by using the Bonferroni correction method (highly specific) and the false discovery rate (FDR) method (highly sensitive). Significantly correlated gene pairs (adjusted $P < 0.05$) are indicated by shading. Tissue categories without any significant correlations are not displayed. All correlations determined to be significant by using the Bonferroni method (darker shading) are significant by using the FDR method (lighter shading). Transcript levels of HAI-1, the proposed endogenous inhibitor of MT-SP1, are significantly correlated with transcript levels of MT-SP1 in the largest proportion of tissues.

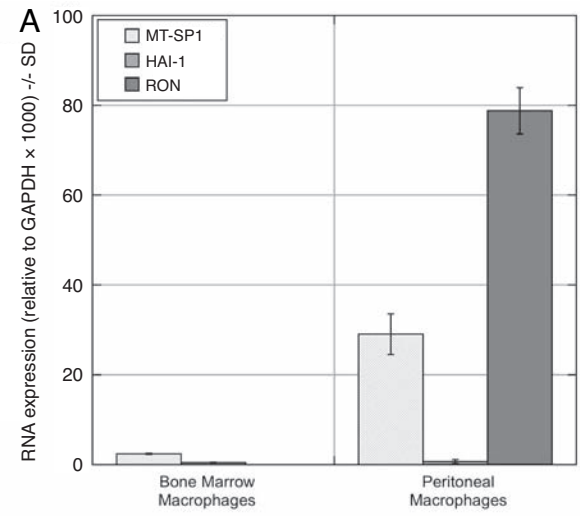

Fig. 2. MT-SP1 and RON, but not HAI-1, are expressed in peritoneal macrophages, and MT-SP1 cleaves MSP-1 at the activation site. (*A*) TaqMan was performed to determine MT-SP1, RON, and HAI-1 expression in primary mouse bone marrow-derived macrophages and peritoneal macrophages. MT-SP1 and RON are expressed at levels at least 10-fold greater in peritoneal macrophages than in bone marrow-derived macrophages. HAI-1 is not expressed in either cell type. (*B*) One hundred nanomolar MT-SP1 was incubated with 200 ng of pro-MSP-1 for 30 min at 37°C and then separated by SDS/PAGE. Approximately 50% of pro-MSP-1 is processed into the active α-β heterodimer in this time, as judged by silver stain. Decrease of the intensity of the pro-MSP-1 band is accompanied by a concomitant increase in the intensity of the band representing the β chain of MSP-1. (*C*) MT-SP1 activates pro-MSP-1 in a dose-dependent manner as is shown by disappearance of the full-length pro-MSP-1 by immunoblot (from left to right: 1 nM, 10 nM, and 100 nM).

with coexpression strength on par with MT-SP1/Trask and MT-SP1/HAI-1. The MT-SP1/MSP-1/RON interaction was chosen for subsequent biochemical validation.

MT-SP1 Is Present on the Cell Surface of Peritoneal Macrophages. Quantitative RT-PCR (Fig. 2) and immunoblotting (data not shown) demonstrated the expression of both MT-SP1 and RON in mouse peritoneal macrophages at levels >10-fold higher than in bone marrow-derived macrophages (Fig. 2). The endogenous inhibitor of MT-SP1, HAI-1, was not highly expressed in either cell type. MSP-1 and RON were originally described as important components of signaling cascades at the surface of certain populations of mature and differentiated macrophages. Previous studies have identified a cell-surface, trypsin-fold serine protease activity on macrophages that activates MSP-1, potentiating MSP-1 binding to RON and subsequent macrophage activation (18–20).

Cell Surface-Bound MT-SP1 Can Cleave the Predicted Substrate pro-MSP-1. We investigated whether MT-SP1 could activate MSP-1 for several reasons: (*i*) MSP-1 requires proteolytic activation to

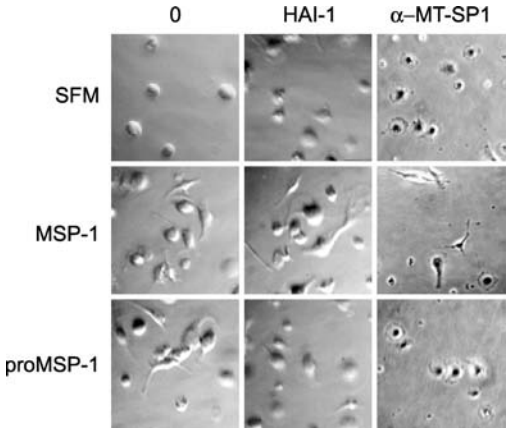

Fig. 3. MT-SP1-activated MSP-1 induces macrophage activation and morphology change. Primary mouse peritoneal macrophages were serum-starved and incubated in serum-free medium (SFM) in the absence or presence of 50 ng/ml MSP-1, 50 ng/ml pro-MSP-1, 40 nM HAI-1, and 400 nM anti-MT-SP1 antibody as indicated for 4 h. Upon treatment with MSP-1 or pro-MSP-1, the macrophages undergo a characteristic morphological change demonstrated by the development of an elongated shape and spiny protrusions. HAI-1 or anti-MT-SP1 antibody inhibition of endogenous MT-SP1 proteolytic activity abrogates the ability of pro-MSP-1 to induce this morphological change.

bind and activate its receptor RON (18–21) (*ii*) MSP-1 contains the consensus sequence for cleavage by MT-SP1 (Table 1), and (*iii*) MT-SP1 and RON are coexpressed in both peritoneal macrophages and cancer tissues, consistent with previous observations that MSP-1 is activated at the surface of cells that respond to MSP-1 (20). Activation of MSP-1 is the result of proteolysis C-terminal to R^{483} (21). The specificity determinant N-terminal to R^{483} is the peptide sequence SKLR (P4-P1) (22), and is in agreement with the PS-SCL results for MT-SP1 (Table 1). MT-SP1 cleaved pro-MSP-1 into two major fragments, which corresponded to the α and β chains of the mature MSP-1 (Fig. 2). Cleavage at R^{483} was confirmed by N-terminal sequencing of the β chain (data not shown). The dose-dependence of this cleavage event was established by analyzing pro-MSP-1 cleavage over a 1,000-fold concentration range. Cleavage of MSP into the α and β chains was detectable at concentrations of protease as low as 1 nM, with nearly complete activation of pro-MSP-1 by 100 nM MT-SP1 within 1 h at 37°C. Activation of RON at R^{309} after the specificity determinant RRRR (P4-P1) was also demonstrated by the nearly complete processing of single chain RON into the mature α/β complex by MT-SP1 (data not shown).

MSP-1 Activation by MT-SP1 Results in Macrophage Morphology Changes and Inhibition of Nitric Oxide Production by Macrophages. The cleavage of MSP-1 by MT-SP1 was then tested in primary cells in culture. Macrophages respond to MSP-1 via RON activation, leading to changes in cell shape and increased migration, as well as an inhibition of nitric oxide production (23–25). We found that primary mouse peritoneal macrophages, but not primary mouse bone marrow macrophages, underwent a characteristic shape change upon activation by MSP-1 (Fig. 3) (25). The effects of the endogenous MT-SP1 inhibitor, HAI-1, and a highly specific MT-SP1 antibody inhibitor (Fig. 3) were studied. The morphology change in response to MSP-1 was independent of HAI-1 or anti-MT-SP1 antibody presence. Both inhibitors were used at concentrations 10-fold over the reported K_i. Cell surface-bound MT-SP1 converted pro-MSP-1 into its biologically active form, and cells underwent morphology change when incubated with pro-MSP-1 in the absence of HAI-1 or the anti-MT-SP1 antibody. Addition of a specific inhibitor of MT-SP1, either HAI-1 or the anti-MT-SP1 antibody, prevented

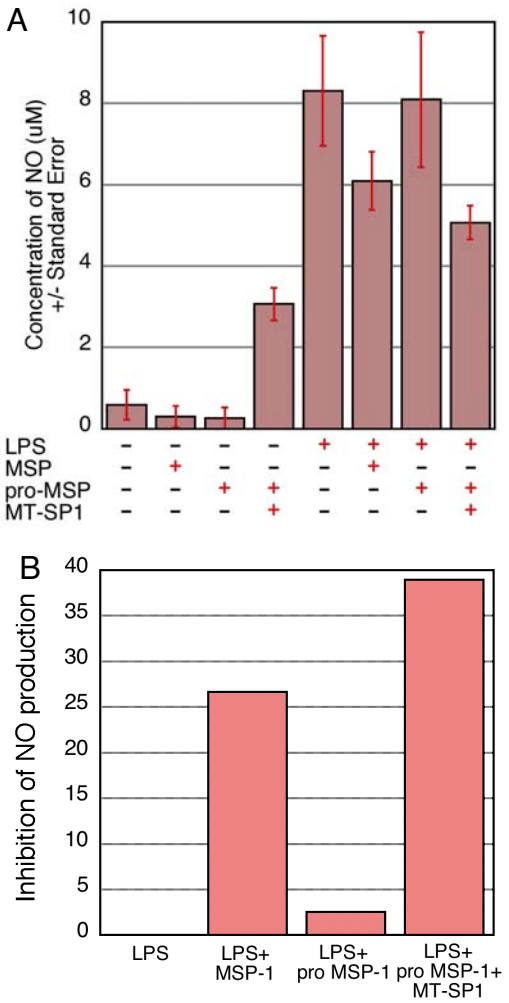

Fig. 4. MT-SP1 activated MSP-1 inhibits LPS-induced nitric oxide production in macrophages. Mouse bone marrow macrophages were isolated and cultured in 24-well plates. Nitric oxide production was measured by the Griess reaction. The macrophages exhibit a robust nitric oxide production response to the positive control of 1 μg/ml LPS. (*A*) From left to right, the histogram represents cell cultured with (*i*) medium alone, (*ii*) 10 ng/ml MSP-1, (*iii*) 10 ng/ml pro-MSP-1, (*iv*) 10 ng/ml pro-MSP-1 plus 10 nM MT-SP1, (*v*) 1 μg/ml LPS, (*vi*) 1 μg/ml LPS plus 10 ng/ml MSP-1, (*vii*) 1 μg/ml LPS plus 10 ng/ml pro-MSP-1, and (*viii*) 10 ng/ml pro-MSP-1 plus 10 nM MT-SP1 plus 1 μg/ml LPS. The experiment was repeated twice in triplicate, and the data from these experiments were averaged and are reported $\pm$SE. (*B*) The data are also presented as percent inhibition of NO production as a function of sample conditions.

macrophage activation despite the presence of pro-MSP-1. These data indicate that MT-SP1, present on the peritoneal macrophage cell surface, is responsible for the activation of pro-MSP-1.

Another measure of macrophage response to MSP-1 is inhibition of LPS-induced nitric oxide production. MSP-1 is a strong attenuator of bone marrow macrophage nitric oxide production in its activated form but does not exhibit this property in its pro-form (23). Primary mouse bone marrow macrophages showed a robust production of nitric oxide in response to LPS (Fig. 4*A*). As expected, pro-MSP-1 alone did not inhibit this response. At baseline, the addition of MT-SP1 alone stimulated production of NO. This is likely secondary to LPS contamination in the recombinant MT-SP1 as it is produced in *Escherichia coli*. However, upon activation of pro-MSP-1 with exogenously added MT-SP1, there was a nearly 40% inhibition of LPS-induced nitric oxide production, commensurate with that achieved with MSP-1 (Fig. 4).

Pro-MSP-1 is thus converted to its bioactive form by MT-SP1, as measured by both macrophage morphology change and inhibition of macrophage nitric oxide production. Furthermore, endogenous MT-SP1 is likely to be responsible for pro-MSP-1 activation on the surface of peritoneal macrophages.

Discussion

Determining the physiological role of orphan proteases has been a long-standing challenge. Many successful approaches have been recently reported by using affinity-tagged mass spectrometric labeling of newly cleaved substrates and through the use of specific macromolecular inhibitors of proteases to identify key components of important cellular pathways (26, 27). Using a strategy combining specificity profiling, transcriptional data, and biochemical enzyme characterization, we have identified a protease (MT-SP1/matriptase), its growth factor substrate (MSP-1), and the corresponding growth factor receptor (RON) as basic components of a cell-stimulatory cascade.

Considering that MT-SP1 could play a significant biochemical role in mediating signaling by processing cancer-related proteins *in vivo*, we hypothesized that these signaling proteins would likely be coexpressed with MT-SP1. To test this hypothesis, a group of candidate genes were chosen whose expression correlated with that of MT-SP1 in cancer tissues. The protein products of these genes were then analyzed for accessible MT-SP1 cleavage motifs. Finally, candidate substrates that were coexpressed with MT-SP1 and had accessible cleavage motifs were validated *in vitro* and in cell-based assays. The coexpression of MT-SP1 with its proposed endogenous inhibitor, HAI-1, provided authentication of our approach. The biological interaction between HAI-1 and MT-SP1 has previously been described in human breast milk (14). Further studies support the interaction of HAI-1 and MT-SP1 in breast cancer tissues, because protein levels of the protease-inhibitor pair are well correlated by immunohistochemistry in a majority of 330 node-negative breast cancer tissue samples (5). Recent work has suggested a role for HAI-1 in both inhibition of MT-SP1 and trafficking of MT-SP1 to the cell surface (28). In our study, MT-SP1 and HAI-1 transcript levels were significantly correlated in a majority of the cancerous tissues examined. This strong correlation suggests that HAI-1 may act as an inhibitor of MT-SP1 in several other types of cancers in addition to the originally shown interaction in breast milk and breast cancer tissue.

Coexpression analysis showed that transcript levels of MT-SP1 and three of its previously described substrates, uPA, PAR2, and Trask, were also significantly correlated in many tissue types. The G protein-coupled receptor PAR2 and the plasminogen activator uPA are both activated by MT-SP1-mediated proteolysis *in vitro*, and some *in vivo* evidence exists to support the physiologic role of MT-SP1 in activating these proteins (29). Recently, Trask/CDCP1/SIMA135, a mitotic substrate of src kinases, was shown to be an endogenous substrate of MT-SP1 (30). Along with HAI-1, Trask was one of the most tightly coregulated proteins identified in the present study. Thus, several PS-SCL-identified substrates of MT-SP1 were coexpressed with MT-SP1, supporting their involvement in MT-SP1-modulated pathways *in vivo*. These data also provide further authentication of the combined substrate specificity/coexpression method for identification of protease substrates. MT-SP1 and a subset of its substrates/inhibitors are coexpressed, and this relationship may be partially generalized to other MT-SP1 substrates and other enzyme-substrate pairs. It is important to note, however, that this approach may not be fully generalized, given that many substrates are expressed distally from the site of enzyme production.

The finding that MT-SP1 and MSP-1 were highly coexpressed supports their physiologic relevance as an enzyme-substrate pair. The interaction was studied in a cell-based system of peritoneal macrophages. We demonstrated that MT-SP1 is expressed on peritoneal macrophages that respond to MSP-1. Although the transcriptional data suggest that HAI-1 and MT-SP1 are often coexpressed, the interaction between HAI-1 and MT-SP1 is likely complex. Peritoneal macrophages represented an ideal system for the study of MT-SP1 because they are primary cells and lack HAI-1, thereby eliminating a possible confounding element to the analysis of cell-based inhibition assays. The exact role of HAI-1 in processes, such as inhibition and trafficking of MT-SP1, however, remains to be determined.

The substrate-specificity profiling data for MT-SP1 is in agreement with its ability to cleave the activation sequence of MSP-1, and this was confirmed *in vitro*. Further experiments demonstrated that cell surface-bound MT-SP1 on peritoneal macrophages activates MSP-1 into its bioactive form and that this constitutive activation could be blocked by the addition of exogenous HAI-1 or a specific antibody inhibitor of MT-SP1. Activation of RON by MSP-1 led to alteration in peritoneal macrophage cell morphology and important downstream biochemical changes such as modulation of NO production in bone marrow-derived macrophages.

Although RON activation by MSP-1 has been thoroughly described in macrophages, resulting in myriad effects ranging from macrophage activation to chemotaxis to proliferation (19), this signaling pathway is also important elsewhere. For example, overexpression of either MT-SP1 or RON, leads to spontaneous tumor formation in mouse models (31, 32). Given this and the data supporting MT-SP1, MSP-1, and RON expression in various cancer tissues, we suggest that this pathway may be important in tumor development, maintenance, and/or progression. MT-SP1, MSP-1, and RON have all been established as cancer-associated molecules (2, 17, 33, 34). We suggest that cancer cells may "hijack" this signaling pathway by increasing coordinate expression of MT-SP1, MSP-1, and RON to drive proliferation and migration, two fundamental traits of transformed cells. The components of this extracellular proteolytic signaling pathway are involved in macrophage activation and are coexpressed in several tumors, suggesting that the cascade may play a critical biological role in certain cell types and many cancer tissues. Their participation in activation of macrophages is particularly interesting, given the association between cancer progression and inflammation (35). The pathway described here may, indeed, have clinical significance, as suggested by a recent study showing that tumors overexpressing MSP-1/MT-SP1/RON are significantly more metastatic than the control group in which only a subset of these genes are expressed (34).

Although this work suggests the sufficiency and importance of MT-SP1 for the activation of MSP-1, MT-SP1 is a member of a much larger family of TTSPs. In certain tissues, these TTSPs may exhibit redundancy of function and may substitute for MT-SP1 in this newly described pathway. Thus, we propose that membrane associated serine proteases, such as, but not limited to, MT-SP1, represent a previously uncharacterized conceptual class of upstream regulators of growth factor activity and thus as catalysts in the initiation of outside-in signaling.

Methods

PS-SCL. Recombinant MT-SP1 was prepared as described (11), and substrate specificity of MT-SP1 was determined by using conditions described in refs. 15 and 36. For further details, please see *SI Methods*.

Tumor Samples, RNA Preparation, and Hybridization to Custom DNA Microarrays. Tumor samples and cell lines were obtained from multiple sources with IRB approval for all tumor samples used in this study. Breast, prostate, and ovarian cancer specimens were obtained from two independent research trials and were therefore analyzed separately and are referred to as trials 1 and 2. Total RNA from nonpathogenic human tissues and organs was obtained commercially (Clontech, Palo Alto, CA; Invitrogen, Carlsbad, CA) or was isolated from fresh-frozen cadaveric samples (Zoion Diagnostics, Shrewsbury, MA) from trauma victims. The details of the tissue samples used and microarray design are more thoroughly described in *SI Methods*.

Quantitative RT-PCR. RNA was extracted from both mouse bone marrow macrophages and peritoneal macrophages by using TRIzol reagent as described elsewhere in this manuscript. The following TaqMan primers were purchased: (Mm00436365_m1 (RON), Mm00487858_m1 (MT-SP1), Mm00444186_m1 (HAI-1) (Applied Biosystems, Foster City, CA). All reactions were performed with Universal PCR Master Mix (Applied Biosystems) using the AB 7300 Real Time PCR system and were monitored over 40 cycles according to manufacturer's recommendations.

Statistical Analysis. Gene expression data were collected for MT-SP1, known substrates, putative substrates, and control genes. To determine the level of correlation of MT-SP1 with these candidate genes, two statistical methods were used. All calculations were performed by using Microsoft Excel or the statistical shareware "R" and are detailed in *SI Appendix*. Pearson's product moment correlation coefficients, Spearman's rank-order correlation coefficients, and associated *P* values were calculated. These *P* values were then corrected by using both the Bonferroni correction and the false discovery rate correction to account for making multiple comparisons (37). Correlation significance was stratified based on the calculated *P* values for both Pearson's and Spearman's correlation calculations. Correlation coefficient pairs and tissue types were clustered and presented in a diagrammatic format. Gene pairs are color coded according to level of significance and sign of the correlation, as described in the figure legend.

Isolation and Culture of Mouse Bone Marrow and Resident Peritoneal Macrophages. Mouse bone marrow macrophages were isolated by flushing the marrow of collected mouse femurs with DMEM and by selection *in vitro* (detailed description in *SI Methods*). Resident peritoneal macrophages were collected from mice by using 10 ml of DMEM or RPMI medium 1640 for peritoneal lavage. Cells were collected by centrifugation and were plated in either DMEM or RPMI medium 1640 with 10% FBS and 1× Pen/Strep. The yield was $\approx 5 \times 10^5$ cells per mouse.

Recombinant MSP-1 Cleavage Reactions. Recombinant human MT-SP1 catalytic domain was prepared and active site titrated as described (11). Recombinant pro-MSP-1 and mature MSP-1 was purchased from R & D Systems (Minneapolis, MN). Briefly, 200 ng of pro-MSP-1 or mature MSP-1 was incubated in the presence or absence of 100 nM MT-SP1 for 30 min at 37°C. This corresponds to a molar ratio of substrate to enzyme of 1.25:1. The products were then separated by SDS/PAGE on 4–20% Tris-glycine gels (Invitrogen) and either silver stained or blotted onto PVDF for microsequencing or nitrocellulose for immunoblotting. N-terminal sequencing of MSP-1 cleavage products was carried out at the University of California Molecular Structure Facility (Davis, CA).

Macrophage Morphology Change Assays. Resident peritoneal mouse macrophages were plated at a density of $\approx 2 \times 10^4$ cells per well in sterile nontissue culture, 24-well plates and cultured in serum-free DMEM overnight. Recombinant MSP-1, pro-MSP-1, HAI-1, and the MT-SP1-specific antibody inhibitor were added to 750 μl of DMEM as indicated in Fig. 3. The antibody

inhibitor was prepared as described and used at a final assay concentration of 400 nM (38). MSP-1 and pro-MSP-1 were used at 50 ng/ml, and HAI-1 was used at 40 nM. Four hundred seventy-five microliters of this culture medium was then applied to the serum-starved cells. After a 1-h incubation at 37°C with 5% CO_2 injection, the cells were analyzed by inverted microscopy, and representative pictures were taken. The experiment was repeated three independent times, and microscopic image acquisition and analysis was blinded.

Testing MT-SP-1 Cleaved MSP-1 for Bioactivity in Nitric Oxide Production Assays. Bone marrow mouse macrophages were isolated as described above and were plated at a density of $\approx 5 \times 10^5$ cells per well in 24-well plates and cultured in serum-free DMEM for 2 h. Recombinant rhMSP-1, pro-MSP-1, MT-SP1, and LPS were added to 750 μl of DMEM as indicated in Fig. 4 and sterile-filtered with a 0.22-μm syringe-driven filter unit (Millipore, Billerica, MA). The final concentration of MSP-1 and pro-MSP-1 was 10 ng/ml, the final concentration of MT-SP1 was 10 nM, and the final LPS concentration was 1 μg/ml. This medium was then added to the cells, and they were cultured for 24 h. After 24 h, nitric oxide production was measured by using the Griess reaction (23). The experiment was performed twice in triplicate. The data were combined and are represented as the average nitric oxide production, with the standard error indicated (Fig. 4*A*). The data are also depicted by condition type as a function of inhibition of NO production (Fig. 4*B*). Percent inhibition of NO production was calculated for each condition as follows. LPS-mediated NO production was established as 0% inhibition. Percent inhibition of NO production for each condition was then calculated as the difference of 100% inhibition and the percentage of NO production in the test sample versus the LPS-alone condition.

We thank R. Roydasgupta and J. Fridlyand of the University of California Comprehensive Cancer Center (San Francisco, CA) for advice and guidance in the use of statistical methods and J. M. Bishop for the use of reagents and facilities at the G. W. Hooper Foundation. This work was supported by the University of California Chancellor's Fellowship, an ARCS Foundation Fellowship, the National Institutes of Health (NIH) Medical Scientist Training Grant (to A.S.B.), a Department of Defense Breast Cancer Research Fellowship (to C.J.F.), and an NIH Program Project Grant (to C.S.C.).

1. Cao J, Zheng S, Zheng L, Cai X, Zhang Y, Geng L, Fang Y (2001) *Chin Med J (English)* 114:726–730.
2. Galkin AV, Mullen L, Fox WD, Brown J, Duncan D, Moreno O, Madison EL, Agus DB (2004) *Prostate* 61:228–235.
3. Hoang CD, D'Cunha J, Kratzke MG, Casmey CE, Frizelle SP, Maddaus MA, Kratzke RA (2004) *Chest* 125:1843–1852.
4. Johnson MD, Oberst MD, Lin CY, Dickson RB (2003) *Exp Rev Mol Diagn* 3:331–338.
5. Kang JY, Dolled-Filhart M, Ocal IT, Singh B, Lin CY, Dickson RB, Rimm DL, Camp RL (2003) *Cancer Res* 63:1101–1105.
6. Oberst MD, Johnson MD, Dickson RB, Lin CY, Singh B, Stewart M, Williams A, al-Nafussi A, Smyth JF, Gabra H, Sellar GC (2002) *Clin Cancer Res* 8:1101–1107.
7. Riddick AC, Shukla CJ, Pennington CJ, Bass R, Nuttall RK, Hogan A, Sethia KK, Ellis V, Collins AT, Maitland NJ, *et al.* (2005) *Br J Cancer* 92:2171–2180.
8. Santin AD, Cane S, Bellone S, Bignotti E, Palmieri M, De Las Casas LE, Anfossi S, Roman JJ, O'Brien T, Pecorelli S (2003) *Cancer* 98:1898–1904.
9. Dhanasekaran SM, Barrette TR, Ghosh D, Shah R, Varambally S, Kurachi K, Pienta KJ, Rubin MA, Chinnaiyan AM (2001) *Nature* 412:822–826.
10. List K, Szabo R, Molinolo A, Sriuranpong V, Redeye V, Murdock T, Burke B, Nielsen BS, Gutkind JS, Bugge TH (2005) *Genes Dev* 19:1934–1950.
11. Takeuchi T, Shuman MA, Craik CS (1999) *Proc Natl Acad Sci USA* 96:11054–11061.
12. Fraser HB, Hirsh AE, Wall DP, Eisen MB (2004) *Proc Natl Acad Sci USA* 101:9033–9038.
13. Miki R, Kadota K, Bono H, Mizuno Y, Tomaru Y, Carninci P, Itoh M, Shibata K, Kawai J, Konno H, *et al.* (2001) *Proc Natl Acad Sci USA* 98:2199–2204.
14. Lin CY, Anders J, Johnson M, Dickson RB (1999) *J Biol Chem* 274:18237–18242.
15. Choe Y, Leonetti F, Greenbaum DC, Lecaille F, Bogyo M, Bromme D, Ellman JA, Craik CS (2006) *J Biol Chem* 281:12824–12832.
16. Friedrich R, Fuentes-Prior P, Ong E, Coombs G, Hunter M, Oehler R, Pierson D, Gonzalez R, Huber R, Bode W, Madison EL (2002) *J Biol Chem* 277:2160–2168.
17. Zhou YQ, He C, Chen YQ, Wang D, Wang MH (2003) *Oncogene* 22:186–197.
18. Skeel A, Leonard EJ (2001) *J Biol Chem* 276:21932–21937.
19. Leonard EJ *Ciba Found Symp* 212:183–191, 1997; discussion 192–197.
20. Wang MH, Skeel A, Leonard EJ (1996) *J Clin Invest* 97:720–727.
21. Wang MH, Yoshimura T, Skeel A, Leonard EJ (1994) *J Biol Chem* 269:3436–3440.
22. Skeel A, Yoshimura T, Showalter SD, Tanaka S, Appella E, Leonard EJ (1991) *J Exp Med* 173:1227–1234.
23. Wang MH, Cox GW, Yoshimura T, Sheffler LA, Skeel A, Leonard EJ (1994) *J Biol Chem* 269:14027–14031.
24. Wang MH, Dlugosz AA, Sun Y, Suda T, Skeel A, Leonard EJ (1996) *Exp Cell Res* 226:39–46.
25. Wang MH, Julian FM, Breathnach R, Godowski PJ, Takehara T, Yoshikawa W, Hagiya M, Leonard EJ (1997) *J Biol Chem* 272:16999–17004.
26. Tam EM, Morrison CJ, Wu YI, Stack MS, Overall CM (2004) *Proc Natl Acad Sci USA* 101:6917–6922.
27. Zhou Q, Snipas S, Orth K, Muzio M, Dixit VM, Salvesen GS (1997) *J Biol Chem* 272:7797–7800.
28. Oberst MD, Chen LY, Kiyomiya KI, Williams CA, Lee MS, Johnson MD, Dickson RB, Lin CY (2005) *Am J Physiol Cell Physiol* 289:C462–C470.
29. Takeuchi T, Harris JL, Huang W, Yan KW, Coughlin SR, Craik CS (2000) *J Biol Chem* 275:26333–26342.
30. Bhatt AS, Erdjument-Bromage H, Tempst P, Craik CS, Moasser MM (2005) *Oncogene* 24:5333–5343.
31. Chen YQ, Zhou YQ, Fu LH, Wang D, Wang MH (2002) *Carcinogenesis* 23:1811–1819.
32. List K, Haudenschild CC, Szabo R, Chen W, Wahl SM, Swaim W, Engelholm LH, Behrendt N, Bugge TH (2002) *Oncogene* 21:3765–3779.
33. Chen YQ, Zhou YQ, Fisher JH, Wang MH (2002) *Oncogene* 21:6382–6386.
34. Welm AL, Sneddon JB, Taylor C, Nuyten D, van de Vijver M, Hasegawa BH, Bishop MJ *Proc Natl Acad Sci USA*, in press.
35. Coussens LM, Werb Z (2002) *Nature* 420:860–867.
36. Harris JL, Backes BJ, Leonetti F, Mahrus S, Ellman JA, Craik CS (2000) *Proc Natl Acad Sci USA* 97:7754–7759.
37. Benjamini Y, Hochberg Y (1995) *J R Stat Soc* 57:289–300.
38. Sun J, Pons J, Craik CS (2003) *Biochemistry* 42:892–900.